by Valery V. Chernykh[1], Charles M. Henderson[2]*, Ruslan V. Kutygin[3], Tatiana V. Filimonova[4], Guzal M. Sungatullina[5], Marina S. Afanasieva[6], Tatiana N. Isakova[7], Rafael Kh. Sungatullin[5], Michael H. Stephenson[8], Lucia Angiolini[9], and Boris I. Chuvashov[4]

Global Stratotype Section and Point (GSSP) for the base-Artinskian Stage (Lower Permian)

[1] Zavaritskii Institute of Geology and Geochemistry, Ural Branch, Russian Academy of Sciences, Pochtovyi per. 7, Yekaterinburg, 620219, Russia
[2] Department of Geoscience, University of Calgary, Calgary, Alberta, Canada T2N 1N4; *Corresponding author, E-mail: cmhender@ucalgary.ca*
[3] Diamond and Precious Metal Geology Institute, Siberian Branch of the Russian Academy of Sciences (DPMGI SB RAS), Lenina ave., 39, Yakutsk, 677007, Russia
[4] Geological Institute of the Russian Academy of Sciences (GIN RAS), Pyzhevsky lane, 7, Moscow, 119017, Russia
[5] Kazan Federal University (KFU), Kremlyovskaya str, 18, Kazan 420008, Russia
[6] Paleontological Institute of Russian Academy of Sciences (PIN PAS), Profsoyuznaya, str. 123, Moscow, 117647, Russia
[7] Geological Institute of the Russian Academy of Sciences (GIN RAS), Pyzhevsky lane, 7, Moscow, 119017, Russia
[8] Stephenson Geoscience Consulting Ltd., 14 Thelda Avenue, Keyworth, Nottingham, NG125HU, UK; British Geological Survey, Keyworth, Nottingham, NG12 5GG, UK
[9] Dipartimento di Scienze della Terra "A. Desio", Università degli Studi di Milano, 20133 Milano, Italy

Editor's Note: The publication of this article with the Russian co-authors is necessary to ensure that the non-Russian co-authors receive publication credit for their valuable contributions to this long-ratified GSSP proposal.

The base-Artinskian Stage GSSP is defined at 0.6 m above the base of bed 4b at the Dal'ny Tulkas section in the southern Urals of Russia (53.88847N and 056.51615E). This point corresponds to the First Appearance Datum of the conodont Sweetognathus asymmetricus, *which is part of a well-defined and widely distributed lineage. Additional markers for correlation include a radioisotopic age interpolated between 290.1 and 290.5 Ma, a strontium isotopic ratio of .70767, and many additional fossils groups, particularly ammonoids and fusulines, but also including small foraminiferans, radiolarians, and palynomorphs. Finally, the boundary occurs within a transgressive succession, near, or at a maximum flooding surface in many sections, thereby forming a distinctive sequence stratigraphic signature in the field. The Artinskian Stage is the third stage of the Lower Permian or Cisuralian Series.*

Introduction

Considerable new data have been generated and understanding significantly improved regarding a potential GSSP level for the base-Artinskian since the reports provided in *Permophiles* 41 (Chuvashov et al., 2002a, b) and *Permophiles* 58 (Chuvashov et al., 2013). Work focused on the Dal'ny Tulkas Section in Russia and the FAD position of *Sweetognathus* aff. *whitei*, but the uncertain taxonomy delayed

final completion; careful study resolved this issue. The taxon is very distinct and an appropriate marker for the base-Artinskian. Kotlyar et al. (2016) showed additional progress at Dal'ny Tulkas, as did Chernykh (2020) and Henderson (2020) indicated that the base-Artinskian GSSP was ready to go. Henderson and Chernykh (2021) reported in *Permophiles* 70 that the key marker species is the conodont *Sweetognathus asymmetricus* Sun and Lai. A series of votes demonstrated overwhelming support for the base-Artinskian GSSP proposal at 0.6 metres above the base of bed 4b at the Dal'ny Tulkas section in the southern Urals of Russia. SPS voting members voted 15-1 (with one non-vote) in favour (see *Permophiles* 72). ICS voted 18-1 in favour (with one non-vote). Finally, on February 2, 2022 the IUGS Executive Committee communicated that they unanimously ratified the proposal. The GSSP is now on the current version of the International Chronostratigraphic Chart. The Dal'ny Tulkas section is data-rich, making it an excellent GSSP site with ammonoids, fusulines, small foraminiferans, palynology, radiolarians, geochronologic ages, and Sr isotopic data that provide additional constraints on how to correlate the GSSP into other regions and realms.

Historical Considerations and Lithologic Succession

The boundary deposits of Sakmarian and Artinskian are represented most fully by the section in the stream Dal'ny Tulkas, located on the southern end of the Usolka anticline near the eastern outskirts
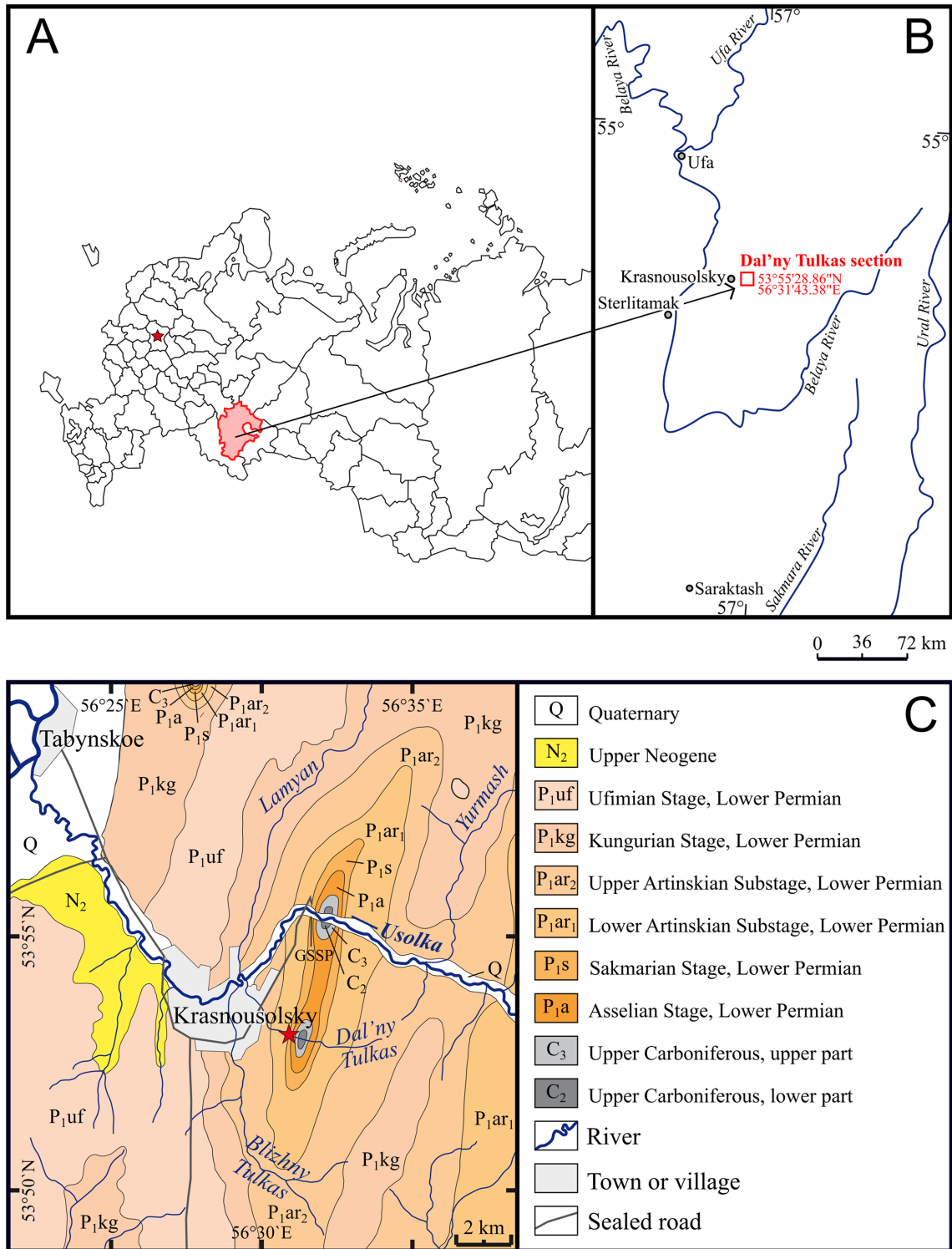
Figure 1. *Geology location map of the Dal'ny Tulkas section. Base of section is 53.88847°N and 056.51615°E.*

of the settlement Krasnousol'sky, Bashkortostan (Fig. 1). The Kurort suite includes predominantly the Sterlitamakian horizon of Sakmarian Stage and the Tulkas suite includes the Artinskian Stage (Chuvashov et al., 1990) within the Dal'ny Tulkas section boundary interval. The Kurort suite comprises beds of dark-coloured carbonate mudstone, argillite, sandstone, and occasional bioclastic limestone with fusulines, rare ammonoids, radiolarians, palynology, and a few bivalves.

The Sterlitamakian horizon is transitional to the Artinskian Stage and is typically poorly exposed. In 2003 a bulldozer cleared this part of the section and exposed all the beds (Fig. 2), which include resistant beds of sandy-argillaceous limestone with rare interbeds of detrital limestone and carbonate-clay concretions; all beds have been sampled for fusulines, ammonoids and conodonts. Most of the conodont samples of the Dal'ny Tulkas section proved to be productive. In the
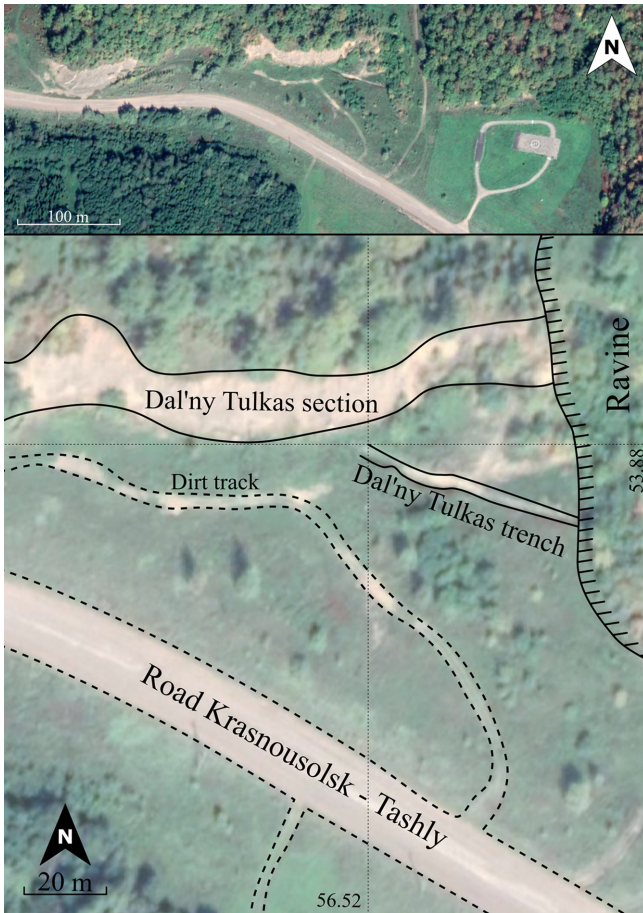
Figure 2. Air photo of the Dal'ny Tulkas section and trench.

Artinskian part of the section there are four ash tuff layers.

The base of the Artinskian Stage is marked by the level of the appearance in bed 4b of the cosmopolitan conodont *Sweetognathus asymmetricus* in the phylogenetic lineage – *Sw. expansus* to *Sw.* aff. *merrilli* to *Sw. binodosus* to *Sw. anceps* to *Sw. asymmetricus* to *Sw. clarki*. The first Artinskian assemblage of fusulines occurs 2.5 m higher in the lower part of bed 5, which also includes Artinskian ammonoids and conodonts. The first appearance datum (FAD) of *Sw. asymmetricus* marks the boundary in the Dal'ny Tulkas section, but everywhere else, the base-Artinskian will be correlated primarily with various fossils including conodonts, as well as a variety of non-biologic stratigraphic signals including radioisotopic ages and strontium isotopes.

The schematic lithologic column of the Dal'ny Tulkas section with indications of the paleontological samples is given below (Figs. 3-4), including detailed description and lists of identified ammonoids, fusulines, conodonts, small foraminiferans and radiolarians (Table 1). There is also an illustration of a trench, which is well correlated and only about 30 metres from the main section (Figs. 2, and 5-6). The correlation between the trench and main section (Fig. 7) is based on lithology and fossil content. The bed numbers and description of the main section and trench vary somewhat because different teams measured the respective sites and because fresh beds, especially for muddy lithology, vary in appearance from the same beds when weathered. The trench was dug to recover fresh

lithologic material and additional fossils; it was not dug to test correlation or provide additional conodont samples, but rather to enrich the paleontological characteristics of the interval, mostly of radiolarians and palynomorphs. Many sections in the world, especially all those from the terrestrial realm, will be correlated without conodonts.

Section Description

Sakmarian Stage - Sterlitamakian Horizon

Kurort suite

Bed 1. Monotonous silty mudstone, grey on fresh fractures, brownish-grey on altered surfaces, microlayered (2 to 5 cm-thick). Fossil content: rare ammonoids, fish-scales, non-calcareous algae. Thickness: 3 m.

Bed 2. Calcareous clayey siltstone and fine-grained sandstone in 15-20 cm-thick beds. Fossil content: noncalcareous algae and plant remains. Thickness: 1.7 m.

Bed 3. Brownish-grey limestone in 10-15 cm-thick beds with mudstone in the middle part of the bed. Carbonate concretions in the upper part of the bed. Fossil content: unidentified radiolarians, rare unidentifiable fusulines, conodonts [*Sweetognathus* cf. *obliquidentatus* (Chernykh)]. Thickness: 0.7 m.

Bed 4a. Monotonous brownish-dark grey platy mudstone, with some interbeds of siltstone. In the lower part of the layer, there are 5-7 cm-thick beds of recessive bioclastic limestone with fusulines (*Pseudofusulina callosa* Rauser, *P. callosa proconcavutas* Rauser, *P. jaroslavkensis fraudulenta* Kireeva, *P.* cf. *parajaroslavkensis* Kireeeva, *P. blochini* Korzhenevski), unidentified radiolarians, bryozoans, crinoids, and conodonts [*Mesogondolella bisselli* (Clark and Behnken), *Sweetognathus anceps* Chernykh, *Sw. obliquidentatus* (Chernykh)], transitional forms from *Sw. anceps* Chernykh to *Sw. asymmetricus* Sun and Lai]. Thickness: 1.8 m.

Artinskian Stage-Burtsevian Horizon

Kurort suite

Bed 4b. Mudstone with carbonate concretions at 0.6 m with conodonts [*Mesogondolella bisselli* (Clark and Behnken), *Sweetognathus anceps* Chernykh., transitional forms from *Sw. anceps* Chernykh to *Sw. asymmetricus* Sun and Lai, *Sw. asymmetricus* Sun and Lai]. 1.2 m above along the section, a level with small carbonate concretions yields conodonts [*Mesogondolella bisselli* (Clark and Behnken), *Sw. obliquidentatus* (Chernykh), *Sw. asymmetricus* Sun and Lai]. The upper part of the unit consists of a 42 cm-thick tempestite composed of coarse-grained graded bed of bioclastic limestone with fusulines (*Pseudofusulina* aff. *longa* Kireeva, *P. fortissima* Kireeva, *P. anostiata* Kireeva, *P. plicatissima* Rauser, *P. urdalensis abnormis* Rauser), bryozoans, crinoids, conodonts [*Mesogondolella bisselli* (Clark and Behnken), *Sw. obliquidentatus* (Chernykh)]. Concretions with unidentified radiolarians. Thickness: 2.6 m.

Figure 3. Stratigraphic column with distribution of samples collected for conodonts, ammonoids, fusulines, and radiolarians in the Dal'ny Tulkas section. See legend for lithology and fossil symbols.

Figure 4. Photo of the upper part of the Dal'ny Tulkas section. The arrow indicates bed 8. The excavated lower part with the GSSP is shown in a later figure.

Tulkas suite

Bed 6. Dark-greenish-grey claystone with carbonate concretions and with 20 cm-thick interbeds of bluish- grey mudstone, locally bioclastic at the top. Fossil content: ammonoids [*Daraelites elegans* Tchernow, *Neopronorites* sp., *Artinskia artiensis* (Grünewaldt), *Medlicottia* sp., *Thalassoceras gemmellaroi* Karpinsky, *Uraloceras* sp., *Paragastrioceras* sp., *Eothinites* sp., *Kargalites* sp., and *Popanoceras annae* Ruzhencev], conodonts [*Mesogondolella bisselli* (Clark and Behnken)]. Thickness: 3.2 m.

Bed 7. Claystone, dark-brownish-grey on fresh fracture, greenish-grey on altered surface, with thin interbeds of marly limestone in the upper part. At 1.1 m below the top of the unit a large (0,5 × 20 cm) concretion of mudstone yields numerous unidentified radiolarians (in sections) and conodonts [*Mesogondolella bisselli* (Clark and Behnken)]. Concretions in the lower part of the bed contain ammonoids [*Daraelites elegans* Tchernow, *Neopronorites* sp., *Medlicottia* sp., *Uraloceras* sp., *Eothinites* sp., *Kargalites* sp.]. Thickness: 5 m.

Bed 8. Limestone, bluish-grey on fresh fractures, whitish on altered

surfaces, locally bioclastic. In the lower 20 cm, 4 cm-thick clayey interbeds occur. At the base and top of the bed, yellowish silicified tuffs up to 10 cm-thick.

Fossil content: ammonoids [*Daraelites elegans* Tchernow, *Neopronorites permicus* (Tchernow), *Neopronorites* sp., *Artinskia artiensis* (Grünewaldt), *Medlicottia orbignyana* (Verneuil), *Medlicottia* sp., *Thalassoceras gemmellaroi* Karpinsky, *Metalegoceras* ex gr. *sogurense* (Ruzhencev), *Uraloceras posterum* Bogoslovskaya and Boiko, *Uraloceras* sp., *Paragastrioceras* sp., *Eothinites* sp., *Kargalites typicus* (Ruzhencev), *Waagenina subinterrupta* (Krotow)]. Thickness (decreasing westwards): 0.7- 0.5 m.

Bed 9. Claystone with periodically repeated (about every 1-2.5 m) 5-10 cm-thick interbeds of steel-grey marly limestone and frequent yellowish-light grey 1-5 cm-thick silicified tuffs. Lenticular concretions of steel-grey marly limestone. In the middle part of the bed, one of the concretions yields numerous unidentified radiolarians (in sections) and conodonts [*Mesogondolella bisselli* (Clark and Behnken)]. Thickness: 9.4 m.

Artinskian Stage - Irginian Horizon

Bed 10. Claystone as below, but with more frequent and thicker (15-20 cm) limestone interbeds and concretions and bioclastic limestone accompanied by 3-10 cm-thick yellowish-light grey silicified tuffs. Fossil content: unidentified radiolarians (in sections), conodonts [*Sweetognathus asymmetricus* Sun and Lai, *Sw. clarki* (Kozur), *Sw.* aff. *binodosus* Chernykh, *Mesogondolella bisselli* (Clark and Behnken), and *M. laevigata* Chernykh]. Thickness: 8.3 m.

Bed 11. Claystone with rare small carbonate concretions. Thickness: 1.7 m.

Trench Description

Sakmarian Stage - Sterlitamakian Horizon

Bed 1. Sandy siltstone, grey, unevenly thin-bedded, with interbeds of clayey mudstone, with a large amount of scattered bioclasts. Fossil content: conodonts (*Mesogondolella* sp.). Thickness: 0.6 m.

Bed 2. Sandy siltstone, microlayered, separated by interbeds of claystone; in the lower part the bedding is poorly expressed, at the top the bedding is very thin. Fossil content: abundant unidentified radiolarians and algae. Thickness: 2.1 m.

Bed 3. Sandy siltstone, grey, microlayered with interbeds of clayey

Table 1. Distribution list of conodonts, ammonoids, fusulinids, and radiolarians from the Dal'ny Tulkas section and trench

Section	Conodonts	Ammonoids	Fusulines
Bed 13	*Sweetognathus clarki* (Kozur), *Sw. asymmetricus* Sun & Lai, *Sweetognathus* aff. *ruzhencevi*, *Mesogondolella bisselli* (Clark & Behnken)		
Bed 10	*Sweetognathus clarki* (Kozur), *Sw. asymmetricus* Sun & Lai, *Sweetognathus* aff. *binodosus*, *Sw.* aff. *clarki*, *Mesogondolella laevigata* Chernykh; base Irginian		
Bed 9	*Mesogondolella bisselli* (Clark & Behnken); top Burtsevian	*Neopronorites* sp., *Waagenina* sp.	
Bed 8		*Daraelites elegans* Tchernow, *Neopronorites permicus* (Tchernow), *Neopronorites* sp., *Artinskia artiensis* (Grünewaldt), *Medlicottia orbignyana* (Verneuil), *Medlicottia* sp., *Thalassoceras gemmellaroi* Karpinsky, *Metalegoceras* ex gr. *sogurense* (Ruzhencev), *Uraloceras posterum* Bogoslovskaya & Boiko, *Uraloceras* sp., *Paragastrioceras* sp., *Eothinites* sp., *Kargalites typicus* (Ruzhencev), *Waagenina subinterrupta* (Krotow) Baigendzhinian	
Bed 7	*Mesogondolella bisselli* (Clark & Behnken)	*Daraelites elegans* Tchernow, *Neopronorites* sp., *Medlicottia* sp., *Uraloceras* sp., *Eothinites* sp., *Kargalites* sp.	
Bed 6	*Mesogondolella bisselli* (Clark & Behnken)	*Daraelites elegans* Tchernow, *Neopronorites* sp., *Medlicottia* sp., *Uraloceras* sp., *Eothinites* sp., *Kargalites* sp.	
Bed 5	*Sweetognathus gravis* Chernykh, *Sweetognathus obliquidentatus* (Chernykh), *Sweetognathus asymmetricus* Sun & Lai, *Mesogondolella bisselli* (Clark & Behnken)	*Popanoceras annae* Ruzhencev, *P. tschernowi* Maximova, *P. congregale* Ruzhencev, *Kargalites* sp. and *Neopronorites skvorzovi* (Tchernow), rare *Artinskia* sp. Aktastinian	*Pseudofusulina callosa* Rauser, *P. plicatissima* Rauser, *P. plicatissima irregularis* Rauser, *P. urdalensis* Rauser, *P. fortissima* Kireeva, *P. concavutas* Vissarionova, *P. juresanensis* Rauser, *P. consobrina* Rauser, *P. paraconcessa* Rauser
Bed 4b	Upper part - *Sweetognathus obliquidentatus* (Chernykh), *Mesogondolella bisselli* (Clark & Behnken) 1.2 m - *Sweetognathus obliquidentatus* Chernykh, *Sweetognathus asymmetricus* Sun & Lai, *Mesogondolella bisselli* (Clark & Behnken) 0.6 m - *Sweetognathus anceps* Chernykh, transitional form between *Sweetognathus anceps* and *Sweetognathus asymmetricus* Sun & Lai, *Sweetognathus asymmetricus* Sun & Lai, *Mesogondolella bisselli* (Clark & Behnken); base Burtsevian		*Pseudofusulina* aff. *longa* Kireeva, *P. fortissima* Kireeva, *P. anostiata* Kireeva, *P. plicatissima* Rauser, *P. urdalensis abnormis* Rauser
Bed 4a	*Sweetognathus obliquidentatus* (Chernykh), *Sweetognathus anceps* Chernykh, transitional form between *Sweetognathus anceps* and *Sweetognathus asymmetricus* Sun & Lai, *Mesogondolella bisselli* (Clark & Behnken); top Sterliltamakian		*Pseudofusulina callosa* Rauser, *P. callosa proconcavutas* Rauser, *P. jaroslavkensis fraudulenta* Kireeva, *P.* cf. *parajaroslavkensis* Kireeva, *P. blochini* Korzhenevski
Bed 3	*Sweetognathus obliquidentatus* (Chernykh)		

Table 1. (continued)

TRENCH	Conodonts	Ammonoids	Fusulines	Small Foraminifers	Radiolarians
Bed 11-6					*Copicyntra fragilispinosa* Kozur & Mostler
Bed 11-3					*Copicyntra fragilispinosa* Kozur & Mostler, *Rectotormentum fornicatum* Nazarov et Ormiston.
Bed 11-2					*Apophysiacus praepycnoclada* (Nazarov & Ormiston), *Apophysiacus sakmaraensis* (Kozur & Mostler), *Astroentactinia inscita* Nazarov in Isakova and Nazarov, *Astroentactinia* sp. G, *Bientactinosphaera* sp. E, *Entactinia dolichoacus* Nazarov in Isakova and Nazarov, *Helioentactinia* sp. C, *Latentifistula heteroextrema* Nazarov in Isakova and Nazarov, *Palaeodiscaleksus* cf. *punctus* (Hinde), *Paratriposphaera strangulate* (Nazarov & Ormiston), *Pluristratoentactinia sp. J*, *Pseudoalbaillella scalprata* Holdsworth & Jones, *Rectotormentum fornicatum* Nazarov & Ormiston, *Seculicollacta amoenitas* Nazarov & Ormiston, *Spongentactinia* sp. A, *Tetragregnon vimineum* Amon, Braun & Chuvashov.
Bed 11-1					*Copicyntra fragilispinosa* Kozur & Mostler
Bed 10	(Bed 10-1) *Eothinites kargalensis* Ruzhencev, *Eothinites* aff. *usvensis* Bogoslovskaya, *Popanoceras annae* Ruzhencev, *P. congregale* Ruzhencev, *Daraelites elegans* Tchernow, *Uraloceras gracilentum* Ruzhencev, *U. involutum* (Voinova), *Crimites* sp., *Aktubinskia* sp.		*Schubertella* aff. *ufimica* Baryshnikov, *?Uralofusulinella* sp.	*Bradyina subtrigonalis* Baryshnikov, *Endothyranella protracta maxima* Baryshnikov, *Tetrataxis lata novosjolovi* Baryshnikov, *Pachyphloia* sp., *Geinitzina richteri kasib* Koscheleva, *Hemigordius* sp., *Nodosinelloides* ex gr. *netchaewi* (Tcherdynzev), *?Uralogordius* sp., *N. jazvae* Kosheleva, *Endothyra rotundata* Morozova, *E. symmetrica* Morozova, *E. lipinae* Morozova, *Pseudoagathammina regularis* (Lipina), *Pseudospira* cf. *vulgaris* (Lipina), *Midiella ovatus minima* (Grozdilova)	*Apophysiacus praepycnoclada* (Nazarov & Ormiston), *Apophysiacus sakmaraensis* (Kozur & Mostler), *Astroentactinia inscita* Nazarov in Isakova and Nazarov, *Astroentactinia* sp. G, *Entactinia dolichoacus* Nazarov in Isakova and Nazarov, *Helioentactinia* sp. B, *Helioentactinia* sp. C, *Latentifistula heteroextrema* Nazarov in Isakova and Nazarov, *Pluristratoentactinia lusikae* Afanasieva, *Spongentactinia* sp. A, *Tetragregnon vimineum* Amon, Braun & Chuvashov.
Bed 9-4		*Popanoceras annae* Ruzhencev			
Bed 9-3					*Copicyntra fragilispinosa* Kozur et Mostler, *Pluristratoentactinia lusikae* Afanasieva.
Bed 9-1					*Copicyntra fragilispinosa* Kozur et Mostler
Bed 8-2			*Boultonia* sp., *Schubertella* sp. A, *Schubertella* sp. B, *S. sphaerica chomatifera* Zolotova, *S. turaevkensis* Baryshnikov, *S. turaevkensis elliptica* Baryshnikov, *S.* ex gr. *kingi* Dunbar & Skinner, *S.* ex gr. *paramelonica* Suleimanov, *Mesoschubertella* sp. 1, *Pseudofusulina* sp. 1, *Pseudofusulina* sp. 2, *P. paraconcessa* Rauser, *P.* ex gr. *pedissequa* Vissarionova, *P. insignita* Vissarionova, *P. abortiva* Tchuvashov, *P. seleukensis* Rauser, *P. urasbajevi* Rauser, *P.* cf. *utilis* Tchuvashov, *P.* cf. *salva* Vissarionova	*Langella* sp., *Dentalina particulata* Baryshnikov, *Hemigordius* sp., *Nodosinelloides incelebrata novosjolovi* (Baryshnikov), *N. netchaewi rasik* (Baryshnikov), *N. bella kamaenis* (Baryshnikov), *N. jaborovensis* (Koscheleva), *Endothyra soshkinae* Morozova, *Bradyina lucida* Morozova, *Pseudobradyina compressa* Morozova, *P. compressa minima* Morozova, *Pseudoagathammina dublicata* (Lipina), *Deckerella elegans* Morozova, *D. elegans multicamerata* Zolotova, *D. media bashkirica* Morozova, *Hemigordiellina elegans* (Lipina), *Postmonotaxinoides costiferus* (Lipina), *Tetrataxis* ex gr. *conica* Ehrenberg, *T. plana* Morozova, *T. hemisphaerica* Morozova, *T. hemisphaerica elongata* Morozova, *T. lata* Spandel, *Lateenoglobivalvulina spiralis* (Morozova), *Trepeilopsis* sp., *Globivalvulina* sp.	
Bed 8-1			*Boultonia* sp., *Schubertella* sp., *Fusiella schubertellinoides* Suleimanov, *Pseudofusulina* sp.	*Dentalina particulata* Baryshnikov, *Geinitzina lysvaensis* Baryshnikov, *G. spandeli* Tcherdynzev, *Nodosinelloides kislovi* (Koscheleva), *N. dualis* (Baryshnikov), *Howchinella* aff. *turae* (Baryshnikov), *Postmonotaxinoides costiferus* (Lipina), *Endothyra lipinae lata* Zolotova, *?Rectoglandulina* sp.	
Bed 7-2					*Apophysiacus praepycnoclada* (Nazarov & Ormiston), *Apophysiacus sakmaraensis* (Kozur & Mostler), *Astroentactinia inscita* Nazarov in Isakova and Nazarov, *Astroentactinia* sp. F, *Astroentactinia* sp. G, *Entactinia chernykhi* Afanasieva & Amon, *Entactinia dolichoacus* Nazarov in Isakova and Nazarov, *Entactinia mariannae* Afanasieva & Amon, *Helioentactinia* sp. B, *Helioentactinia* sp. C, *Helioentactinia* sp. D, *Helioentactinia* sp. I, *Kozurispongus laqueus* (Nazarov & Ormiston), *Latentidiota promiscua* (Nazarov & Ormiston), *Latentifistula heteroextrema* Nazarov in Isakova and Nazarov, *Microporosa permica permica* (Kozur & Mostler), *Nazarovispongus aequilateralis* (Nazarov in Isakova and Nazarov), *Nazarovispongus pavlovi* Kozur, *Pluristratoentactinia* sp. J, *Spongentactinia fungosa* Nazarov, *Spongentactinia* sp. A, *Spongentactinia* sp. H, *Tetragregnon sphaericus* Nazarov in Isakova and Nazarov, *Tetragregnon vimineum* Amon, Braun & Chuvashov.
Bed 5-2					*Copicyntra fragilispinosa* Kozur & Mostler, *Palaeodiscaleksus* cf. *punctus* (Hinde)
Bed 1	*Mesogondolella* sp.				

Figure 5. Stratigraphic column with distribution of samples collected for conodonts, ammonoids, fusulines, and radiolarians in the Dal'ny Tulkas trench. See legend of Fig. 3 for lithology and fossil symbols.

sandstone. Fossil content: calamite trunks, algae, fish scales. Thickness: 1.2 m.

Bed 4. Dark grey, thin-bedded siltstone with an interbed of red tuff at the base. Fossil content: algae, unidentified radiolarians, and fish scales. Thickness: 0.45 m.

Bed 5. Calcareous clayey siltstone with interbeds of fine-grained sandstone and reddish tuffs. Fossil content: fish scales, numerous radiolarians, and algae. Thickness: 1.5 m.

Bed 6. Calcareous sandstone, silty. Thickness: 0.2 m.

Bed 7-1. Grey mudstone, microlayered, platy. Concretions of brown-

Figure 6. Photo of the Dal'ny Tulkas trench section for the Sakmarian-Artinskian boundary interval (person for scale is standing on trench bed 8). The main section is in the background.

ish-grey limestone at the base and the top. Thickness: 1.0 m.

Bed 7-2, 7-3. Mudstone with silty interbeds, brownish-dark grey, platy. In the lower part of the bed, there is a 5-7 cm-thick bed of bioclastic limestone with rare unidentifiable fusulines, bryozoans, crinoids. In 7-2 concretions of limestone with numerous radiolarians Thickness: 0.8 m.

Bed 7-4, 7-5. Silty mudstone, grey, with carbonate nodules. Thickness: 0.8 m.

Artinskian Stage - Burtsevian Horizon

Bed 8. Bioclastic limestone, coarse-grained, interpreted as a tempestite. Fossil content: abundant fusulines (8-1: *Boultonia* sp., *Schubertella* ex gr. *sphaerica* Suleimanov, *Fusiella schubertellinoides* Suleimanov, *Pseudofusulina* ? sp.; 8-2: *Boultonia* sp., *Schubertella* sp. A, *Schubertella* sp. B, *S. sphaerica chomatifera* Zolotova, *S. turaevkensis* Baryshnikov, *S. turaevkensis elliptica* Baryshnikov, *S.* ex gr. *kingi* Dunbar and Skinner, *S.* ex gr. *paramelonica* Suleimanov, *Mesoschubertella* sp. 1, *Pseudofusulina* sp. 1, *Pseudofusulina* sp. 2, *P. paraconcessa* Rauser, *P.* ex gr. *pedissequa* Vissarionova, *P. insignita* Vissarionova, *P. abortiva* Tchuvashov, *P. seleukensis* Rauser, *P. urasbajevi* Rauser, *P.* cf. *utilis* Tchuvashov, *P.* cf. *salva* Vissarionova). Thickness: 0.15 m.

Bed 9. Dark grey mudstone with thin beds of siltstone and numerous limestone nodules. Fossil content: ammonoids (9-4: *Popanoceras annae* Ruzhencev), radiolarians. Thickness: 2.2 m.

Bed 10. Bioclastic limestone, grey, fine-grained, with interbeds of mudstone. Fossil content: large plant remains, fusulines (*Schubertella* aff. *ufimica* Baryshnikov, ?*Uralofusulinella* sp.), radiolarians, brachiopods, ammonoids [10-1: *Eothinites kargalensis* Ruzhencev, *Eothinites* aff. *usvensis* Bogoslovskaya, *Popanoceras annae* Ruzhencev, *P. congregale* Ruzhencev, *Daraelites elegans* Tchernow, *Uraloceras gracilentum* Ruzhencev, *U. involutum* (Voinova), *Crimites* sp., *Aktubinskia* sp.]. Thickness: 0.5 m.

Bed 11. Silty mudstone with nodules and interbeds of grey limestone. Fossil content: radiolarians, plant remains, and brachiopods. Thickness: 2.2 m.

Interpreted Sequence Stratigraphy

The Artinskian succession is associated with a transgressive systems tract and a maximum flooding surface in many global sections (Beauchamp et al., 2022b). This is recognised in the Raanes and Great Bear Cape formations in the Canadian Arctic (Chernykh et al., 2020; Beauchamp et al., 2022a) where the base-Artinskian is correlated to a maximum flooding surface (MFS) and associated with the local first occurrence of *Sweetognathus asymmetricus*. Having the boundary within or at the top (MFS) of a transgressive systems tract provides an easily identified physical stratigraphic correlation tool. The section at Dal'ny Tulkas has not been investigated in detail for the sequence stratigraphy, but it does exhibit features that can be interpreted as a sequence boundary and transgressive systems tract. For example, non-calcareous algae, plant remains, and *Calamites* have been recovered from beds 3 and 4 in the trench and beds 1-3 in the main section; also, bed 6 in the trench comprises calcareous sandstone. Units above bed 2 in the section and bed 6 in the trench (above lowest dashed line in Fig. 7) include carbonate mudstone, with increasingly diverse and abundant marine fossils and a little higher the base-Artinskian boundary is defined at the main section (solid red line in Fig. 7). Sedimentation appears to be uninterrupted throughout this transgressive interval, punctuated only by tempestites that delivered contemporaneous coarser bioclastic material to the slope during storms. The tempestites are a normal feature in most stratigraphic successions and actually enhance the biostratigraphic signal by delivering shallow water bioclasts to the slope setting.
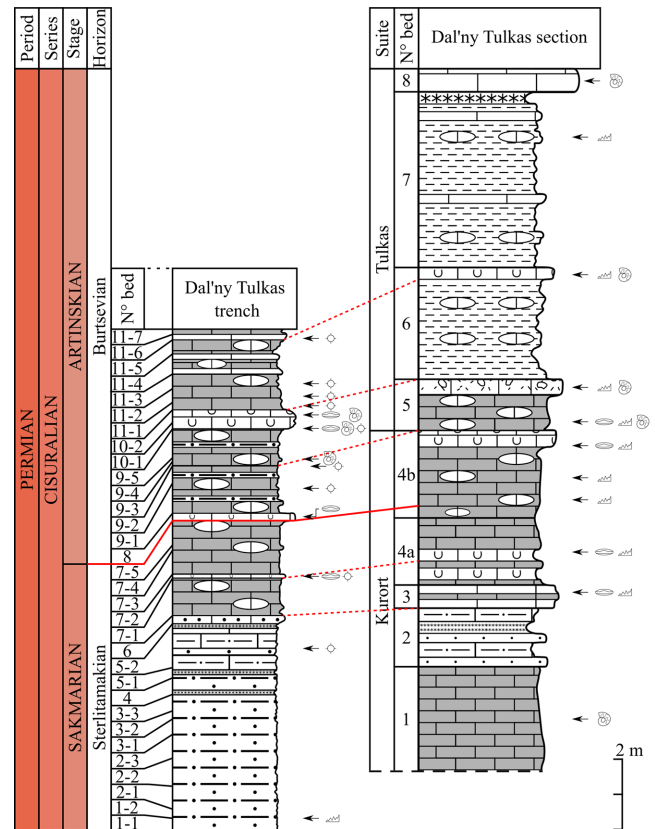
Figure 7. Correlation of the Dal'ny Tulkas section and trench.

Biostratigraphy

The Dal'ny Tulkas section and trench have been studied extensively for biostratigraphic content. The following sections provide details regarding the occurrence and biostratigraphic utility of conodonts, ammonoids, fusulines, small foraminiferans, palynomorphs, and radiolarians.

Conodonts

Conodonts are considered the primary biostratigraphic tool for this interval (Henderson, 2018), which makes it possible to clearly carry out global correlation with the appearance of the cosmopolitan form – *Sweetognathus asymmetricus* Sun and Lai. Its position in the chronomorphocline (Fig. 8) *Sw. binodosus - Sw. anceps - Sw. asymmetricus* is confirmed by the study of the Dal'ny Tulkas section (Henderson and Chernykh, 2021). The Dal'ny Tulkas section provides the best information with respect to conodonts of the genus *Sweetognathus* in the Uralian region (Chernykh, 2005, 2006).

In order to explain the value of these new data, it is useful to consider the previously published information about the development of this group of conodonts in the Usolka section (Chernykh and Chuvashov, 2004). The primitive form, *Sweetognathus expansus* (Perlmutter), in which the beginning of the carinal differentiation (Fig. 8) occurs, appears in middle to late Asselian. In latest Asselian to early Tastubian it evolves into *Sweetognathus* aff. *merrilli* (this form is significantly different from the type *Sw. merrilli* Kozur of mid-Asselian age; see Boardman et al., 2009; Petryshen et al., 2020) with carinal development forming rounded nodes in upper view (Fig. 8). Further evolution of this group leads to the appearance in the Tastubian horizon of forms with fewer carinal nodes, but those nodes are laterally elongated with a tendency toward the bilobate dumbbell-like structure. These forms are referred to *Sweetognathus binodosus* Chernykh (Fig. 8).

Asselian Stage		Sakmarian Stage		Artinskian Stage
Conodont Zone				
postfusus	aff. *merrilli*	*binodosus*	*anceps*	*asymmetricus*
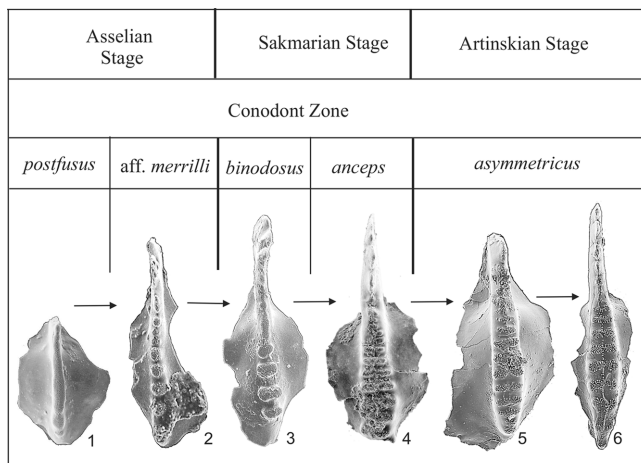
Figure 8. The evolutionary lineage: 1 - **Sweetognathus expansus (Perlmutter), (Usolka section, bed 21); 2 -** **Sw.** *aff.* **merrilli** *Kozur (Usolka section, bed 26/2); 3 -* **Sw. binodosus** *Chern. (Usolka section, bed 26/3); 4 -* **Sw. anceps** *Chern. (Dal'ny Tulkas section, bed 4a); 5 - transitional form from* **Sw.** *anceps to* **Sw.** *asymmetricus* **Sun and Lai** *(Dal'ny Tulkas section, bed 4b); 6 -* **Sw. asymmetricus** *Sun and Lai (Dal'ny Tulkas, bed 4b).*

The evolutionary features of this group during the Sterlitamakian and Artinskian time are revealed at the Dal'ny Tulkas section. The development of the carina on Sterlitamakian representatives of the lineage *Sweetognathus expansus- Sw.* aff. *merrilli - Sw. binodosus* continues in the direction of the differentiation of carinal nodes, which led to the appearance of *Sw. anceps* Chernykh (Fig. 9) that possess dumbbell-like nodes. In addition to these forms, there appear morphotypes that include fragmentary development of the pustulose mid-carinal connecting ridge, which are considered as transitional to *Sw. asymmetricus*. Forms of *Sw. anceps* with the rudiments of mid-carinal pustulose ridge continue to be encountered higher in the section until finally there appear specimens of *Sweetognathus* with fully developed dumbbell-like nodes and a complete middle pustulose connecting ridge. These forms are identified as the species *Sweetognathus asymmetricus* (Figs. 9-10) whose representatives are widely known in many regions where deposits of Artinskian age are present. Proposals to use the appearance of *Sw. asymmetricus* for correlating the lower boundary of the Artinskian Stage were noted previously by different researchers (Kozur, 1977; Ritter, 1986; Wang et al., 1987; Mei et al., 2002). In those reports the taxon was identified as *Sw. whitei,* which is a species now known to be a late Asselian homeomorph (see Rhodes, 1963, Riglos Suarez et al., 1987 and Holterhoff et al., 2013 for examples; problems discussed in Henderson, 2018; lineages discussed in Petryshen et al., 2020). There was insufficient knowledge at the time about the early members of this evolutionary lineage. Forms referred to the species *Sweetognathus anceps*, also occur widely, but until now they were encountered together with the typical *Sw. asymmetricus*, and the majority of researchers identified those specimens, without the fully developed middle connecting ridge to *Sweetognathus* cf. *whitei*. The transitional passage from *Sw. anceps* to *Sw. asymmetricus* is traced for the first time; these transitional forms indicate proximity to the boundary, but the boundary is marked by the FAD of *Sw. asymmetricus*. The evolutionary development of these conodonts within the lineage *Sweetognathus expansus - Sw.* aff. *merrilli - Sw. binodosus - Sw. anceps - Sw. asymmetricus* (Fig. 8) is now completely understood. The emended definition as described by Henderson and Chernykh (2021) for *Sweetognathus asymmetricus* will need to be considered carefully given its importance for correlation of the Artinskian. Some previous correlations will need to be revised. For example, the cyclothem interval from Florence Limestone to Fort Riley Limestone in Kansas (Boardman et al., 2009), long correlated with the Artinskian because of the occurrence of *Sweetognathus whitei*, should now be considered as upper Asselian. The co-occurrence of *Sw. whitei* and *Streptognathodus florensis* in Kansas supports a latest Asselian age; Chernykh (2006) reports *S. florensis* from the Usolka section of Russia exactly 1.1 metre below the GSSP for the base-Sakmarian stage (Chernykh et al., 2020). *Sweetognathus whitei* co-occurs with abundant specimens of *Streptognathodus* (Rhodes, 1963; Boardman et al., 2009) – the latter taxon became extinct near the base of the Sakmarian. Other sections in which this taxonomic distinction is made are described below.

The chronomorphocline *Sw. binodosus - Sw. anceps - Sw. asymmetricus* can also be recognized in transgressive facies of uppermost Raanes and lower Great Bear Cape formations of southwest Ellesmere Island, Canadian Arctic (Henderson, 1988; Beauchamp and Henderson, 1994; Henderson, 1999; Mei et al., 2002; Chernykh et al., 2020; Beauchamp et al., 2022a). It is also recognized in the Riepetown Formation, Moor-
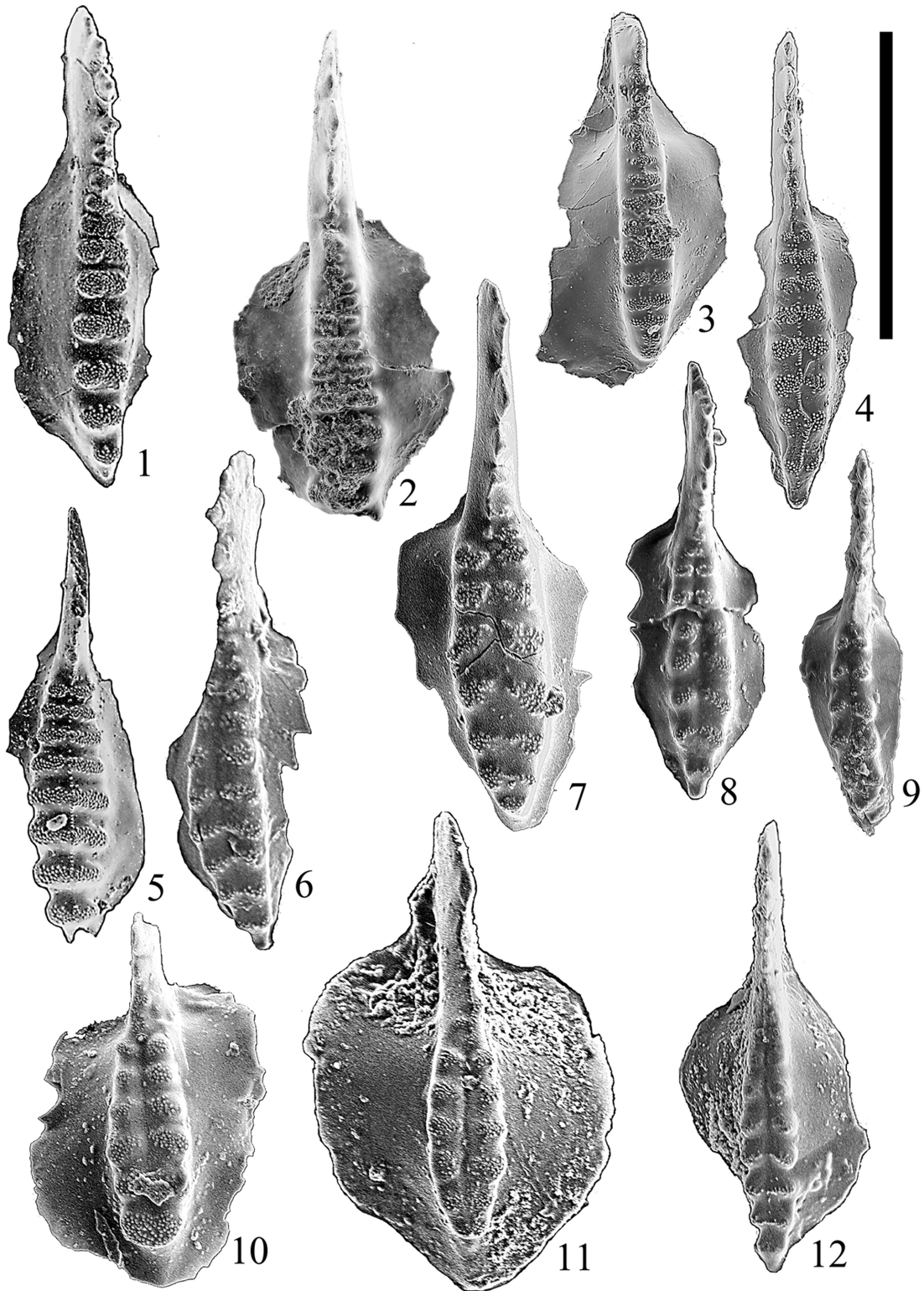
Figure 9. Upper Sakmarian-Lower Artinskian conodonts in Dal'ny Tulkas section (x90). Scale bar: 500 µm. 1, 2. **Sweetognathus anceps** *Chernykh,* *2005: 1 – holotype DT19-1,* **bed 5;** *lower part of Artinskian,* **asymmetricus** *Zone; 2 – DT24,* **bed 4a;** *upper Sakmarian, Sterlitamakian horizon,* **anceps** *Zone. 3-5.* **Sweetognathus asymmetricus** *Sun and Lai, 2017: 3 - DT-18a, transitional form from* **Sweetognathus anceps** *Chernykh to* **Sw. asymmetricus** *Sun and Lai,* **bed 4b;** *4 - DT-18b, typical specimen with a fully developed median ridge,* **bed 4b;** *5 - T-19-3, specimen with* **symmetrical carina,** **bed 5,** *lower part of Artinskian, Burtsevian horizon,* **asymmetricus** *Zone. 6-8.* **Sweetognathus obliquidentatus** *(Chernykh),* *1990: 6 – holotype ZSP-1070/19v; 7 – DT40-3; 8 – T/19-1-5;* **bed 5;** *lower part of Artinskian, Burtsevian horizon,* **asymmetricus** *Zone. 9, 12.* **Sweetog-** **nathus** *aff.* ruzhencevi *(Kozur), 1976: 9 – DT40-6; 12 – DT40-13;* **bed 5;** *lower part of Artinskian, Burtsevian horizon,* **asymmetricus** *Zone. 10, 11.* **Swee-** **tognathus gravis** *Chernykh, 2006: 10 – DT40-10k; 11 – holotype U40-9b; bed 5; lower part of Artinskian, Burtsevian horizon,* **asymmetricus** **Zone.**
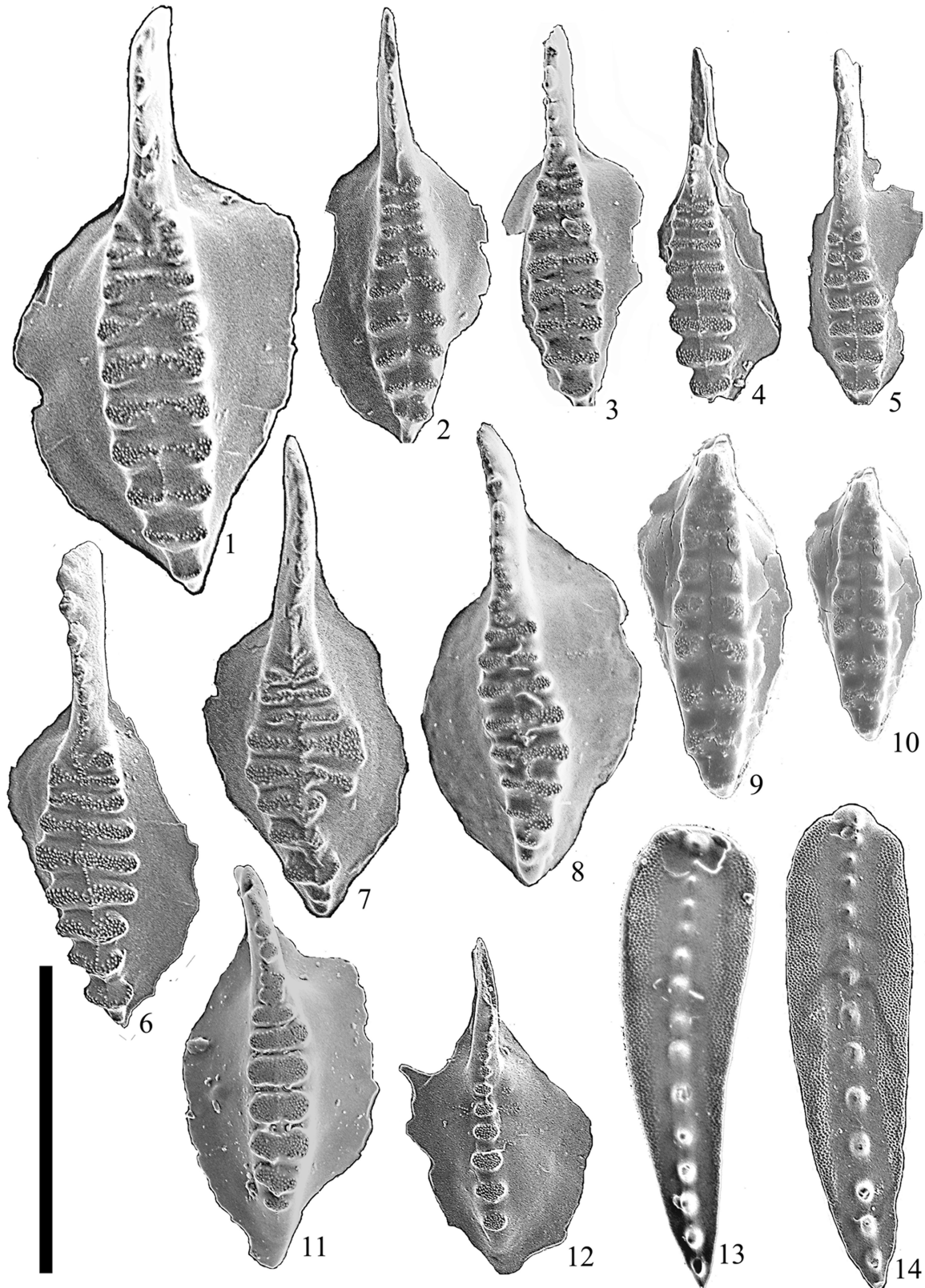
Figure 10. Lower Artinskian conodonts in bed 10 (Artinskian, lower part of Irginian horizon, **clarki** *Zone in Dal'ny Tulkas section (x90). Scale bar: 500 µm. 1, 4-8.* **Sweetognathus asymmetricus** *Sun and Lai, 2017: 1 – DT40-27, the relicts of the longitudinal middle ridge are visible; 4 – DT40-29, the middle ridge is located above upper surface of carinal nodes; 5 – DT40-17, the middle ridge is located lower upper surface of carinal nodes; 6 – DT40-24; 7 – DT40-19; 8 – DT40-21. 2, 3.* **Sweetognathus** *aff.* **clarki** *(Kozur), 1976: 2 – DT40-18; 3 – DT40-22, the relicts of the longitudinal middle ridge are visible. 9, 10.* **Sweetognathus clarki** *(Kozur), 1976: 9 – DT40-33; 10 – DT40-32. 11, 12.* **Sweetognathus** *aff.* **binodosus** *Chernykh, 2005: 11 – DT40-23; 12 – DT40-20. 13, 14.* **Mesogondolella laevigata** *Chernykh, 2005: 13 – U40-26; 14 – holotype DT40-25.*

man Ranch, Nevada (Ritter, 1986), upper Riepe Springs Limestone, Elko County, Nevada (Read and Nestell, 2018), Buckskin Mountain Formation in Carlin Canyon, Nevada (Dehari, 2016; Beauchamp et al., 2022b), Ross Creek Formation in southeastern British Columbia (Henderson and McGugan, 1986), and many other regions. In South China, the chronomorphocline can be recognized in condensed and continuously deposited thin beds of slope carbonates, organic-rich mudstone or shale and wackestone in the Luodian (NSC) and Ziyun (Houhongchong or HHC) sections of Guizhou province (Chen, 2011). These slope deposits are correlated with the Liangshan Formation (or Liangshan Member in the lower part of the Chihsia Formation) and the time represented by a hiatus between the Liangshan Formation and the Maping Formation in more proximal sections in South China. Chen (2011) illustrated well preserved specimens of *Sweetognathus binodosus* and *Sw. anceps* from 347 to 362 metres above the Luodian section base. Wang and Higgins (1989) and Wang (1994) also illustrated *Sw. binodosus* and *Sw. asymmetricus* (as *Sw. whitei*) from the Luodian section. Chen (2011) illustrated *Sw. asymmetricus* (as *Sw. whitei* in his thesis) from -533 to -548 metres at the Houhongchong section in Ziyun. *Sweetognathus asymmetricus* was named for its occurrence in beds 18-23 at the Tieqiao section (Guangxi Province) of south China (Sun et al., 2017). This level is near the lithologic boundary between the Liangshan Member and the lower part of the typical Chihsia Formation and seems to be high in the range of the species (Wang et al., 1987; Zhang et al., 1988; Shen et al., 2007; Sun et al., 2017). The species, as currently understood, may have a long range, but the FAD level of *Sw. asymmetricus* is clearly recognized by being proximal to the *Sw. binodosus-Sw. anceps* lineage, with transitional forms from *Sw. anceps* and *Sw. asymmetricus* overlapping the boundary. At the Dal'ny Tulkas section, *Sw. asymmetricus* ranges at least as high as bed 13 (60 metres above bed 11; see Table 1), where it co-occurs with *Sw. clarki*, *Sw.* aff. *ruzhencevi*, and *Mesogondolella bisselli*.

Ammonoids

Dal'ny Tulkas section

Little was known about the ammonoids of the Dal'ny Tulkas section prior to the boundary studies. Previously, Boris Chuvashov and colleagues made collections at two levels of the lower part of the Artinskian stage (Bed 5), in which M.F. Bogoslovskaya identified *Popanoceras annae* Ruzhencev, P. *tschernowi* Maximova, *P. congregale* Ruzhencev, *Kargalites* sp. and *Neopronorites skvorzovi* (Tchernow) (Chuvashov et al., 2002a, b). This association dates the host beds as early Artinskian (Aktastinian).

In 2016 and 2021, R.V. Kutygin searched for fossil cephalopods in the natural outcrop of the Dal'ny Tulkas and ammonoids were collected from beds 6-9. Ammonoids recovered from beds 6 and 7 include *Daraelites elegans* Tchernow, *Artinskia artiensis* (Grünewaldt), *Thalassoceras gemmellaroi* Karpinsky, *Popanoceras annae* Ruzhencev as well as representatives of the genera *Medlicottia, Uraloceras, Paragastrioceras, Eothinites,* and *Kargalites*. All the listed species are characteristic of both Aktastinian and Baigendzhinian regional stages of the southern Urals (Ruzhencev, 1956).

The richest ammonoid assemblage occurs in Bed 8. It includes *Daraelites elegans* Tchernow, *Neopronorites permicus* (Tchernow), *Neopro-*

norites sp., *Artinskia artiensis* (Grünewaldt), *Medlicottia orbignyana* (Verneuil), *Medlicottia* sp., *Thalassoceras gemmellaroi* Karpinsky, *Metalegoceras* ex gr. *sogurense* (Ruzhencev), *Uraloceras posterum* Bogoslovskaya and Boiko, *Uraloceras* sp., *Paragastrioceras* sp., *Eothinites* sp., *Kargalites typicus* (Ruzhencev), and *Waagenina subinterrupta* (Krotow). This assemblage belongs to the Baigendzhinian regional stage of the southern Urals (but Burtsevian in Fig. 3) based on the presence of *Medlicottia orbignyana*, *Metalegoceras* ex gr. *sogurense*, *Uraloceras posterum* and *Waagenina subinterrupta*.

Clay-carbonate concretions of Bed 9 sometimes contain poorly preserved ammonoids, among which are identified *Neopronorites* sp. and *Waagenina* sp.

Dal'ny Tulkas trench

At 1.6 m above the Sakmarian-Artinskian Stage boundary, a small accumulation of shells of *Popanoceras annae* Ruzhencev occur in clay-carbonate concretions in interbed 9-4 of bed 9 of the trench. This is the most common Artinskian ammonoid of the southern Urals. The vertical interval of distribution of *Popanoceras annae* covers both substages of the Artinskian Stage; however most of the known specimens come from the lower substage (Aktastinian).

In the bioclastic limestone of the trench, many more juvenile ammonoids are scattered 2.5 m above the Sakmarian-Artinskian boundary (bed 10-1 of the trench; Fig. 11; Table 1). Rare medium-sized and large ammonoid specimens are usually represented only by fragments. The collection of cephalopods is dominated by *Eothinites kargalensis* Ruzhencev, which is often found in the Aktastinian of the southern Urals. Among the *Eothinites*, several specimens have prominent transverse ornamentation (Figs. 11.4, 11.5), previously identified as *Eothinites* aff. *usvensis* Bogoslovskaya. Possessing ornamentation very similar to representatives of *E. usvensis* from the Urmy Formation (upper of part Artinskian) of the Middle Urals (Bogoslovskaya, 1962), the Dal'ny Tulkas specimens differ in the less evolute shell. In addition to *Eothinites*, the assemblage contains *Popanoceras annae*, *P. congregale*, and *Daraelites elegans* Tchernow, which characterize the Artinskian Stage of the Urals. Paragastrioceratids are rare; they are represented by small specimens of *Uraloceras involutum* (Voinova) and *U. gracilentum* Ruzhencev.

The species *Uraloceras involutum* is the most common of the Artinskian paragastrioceratids of the southern Urals, with the best finds occurring in the lower substage (Aktastinian). In addition to the southern Urals, this species is also known from the Urmy Formation of the Middle Urals (Bogoslovskaya, 1962), in the Kosva Formation of the Pechora Basin (Bogoslovskaya and Shkolin, 1998), in the upper Raanes ("Assistance") Formation of Ellesmere Island of the Canadian Arctic Archipelago (Nassichuk et al., 1966; Nassichuk, 1975), in the Jungle Creek Formation of the northern Yukon Territory (Nassichuk, 1971), in the Eagle Creek Formation of Alaska (Schiappa et al., 2005), as well as possibly in British Columbia and in Nevada (Schiappa et al., 2005).

A rare Aktastinian species of *Uraloceras gracilentum* has features of the oldest paragastrioceratids, expressed by unusually slow coiling for the genus *Uraloceras*. According to Ruzhencev (1956), the possible ancestor of *Uraloceras gracilentum* is the late Sakmarian species *Uraloceras limatulum* Ruzhencev, which probably belongs to a separate genus from *Uraloceras*. The shells of species of the genera *Crimi-*
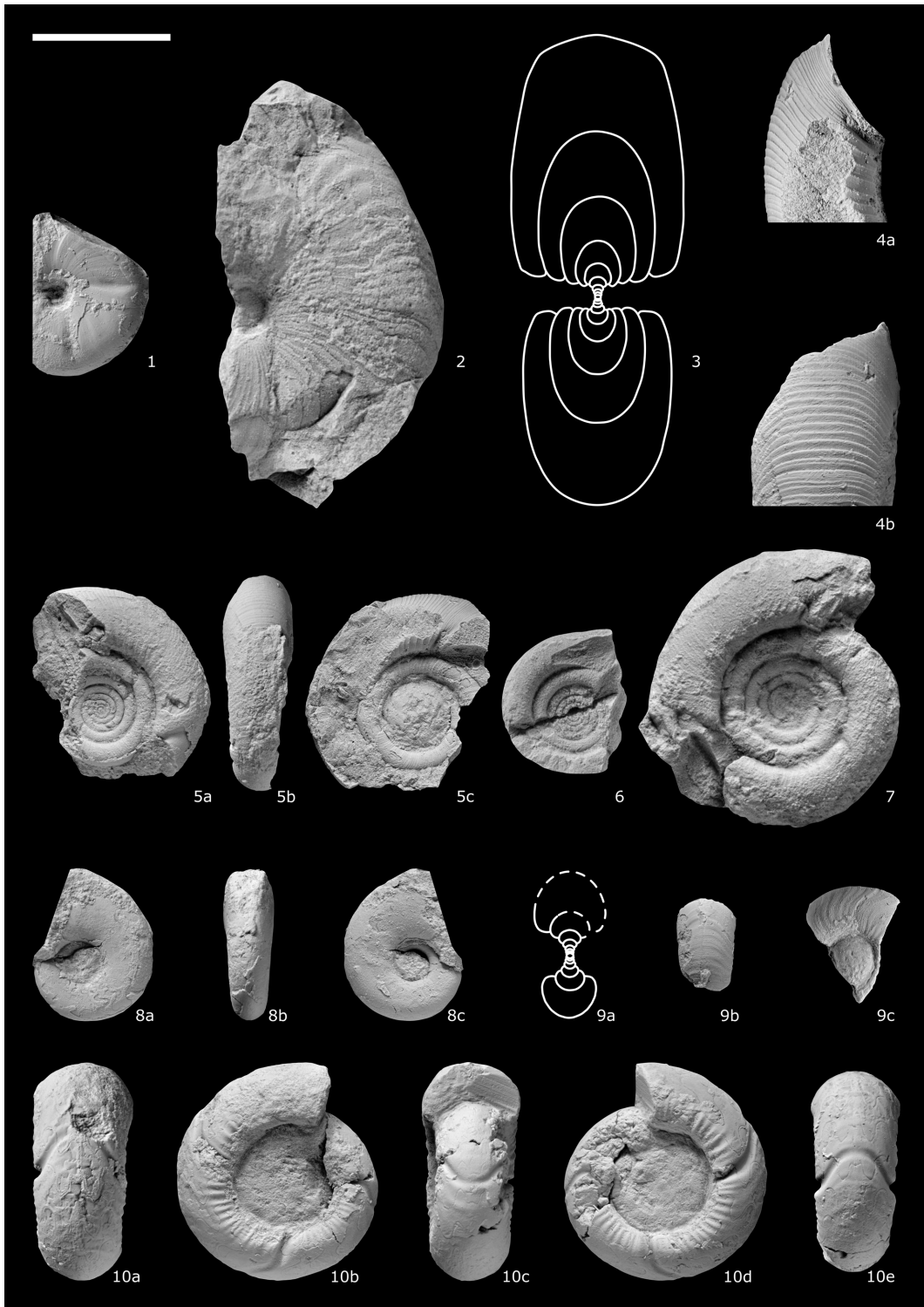
Figure 11. *Ammonoids from the Dal'ny Tulkas trench, beds 9-4 (fig. 2) and 10-1 (figs 1, 3-10). Scale bar: 10 mm for figs 1-3, 5-9; 8.5 mm for fig. 10; 5 mm for fig. 4. 1.* **Popanoceras congregale** *Ruzhencev.* **2-3.** **Popanoceras annae** *Ruzhencev.* **4-5.** **Eothinites** *aff.* **usvensis** *Bogoslovskaya.* **6-7.** **Eothinites kargalensis** *Ruzhencev.* **8.** **Daraelites elegans** *Tchernow.* **9.** **Uraloceras involutum** *(Voinova).* **10.** **Uraloceras gracilentum** *Ruzhencev.*

tes and *Aktubinskia* have also been found here, but poorly preserved.

It follows from the above that in the Dal'ny Tulkas section, there is a change from the Aktastinian to the Baigendzhinian ammonoid association. The biostratigraphic utility of Permian ammonoids is summarized in Leonova (2018).

Foraminiferans

Dal'ny Tulkas section

Fusulines occurring with Sakmarian conodonts are represented by
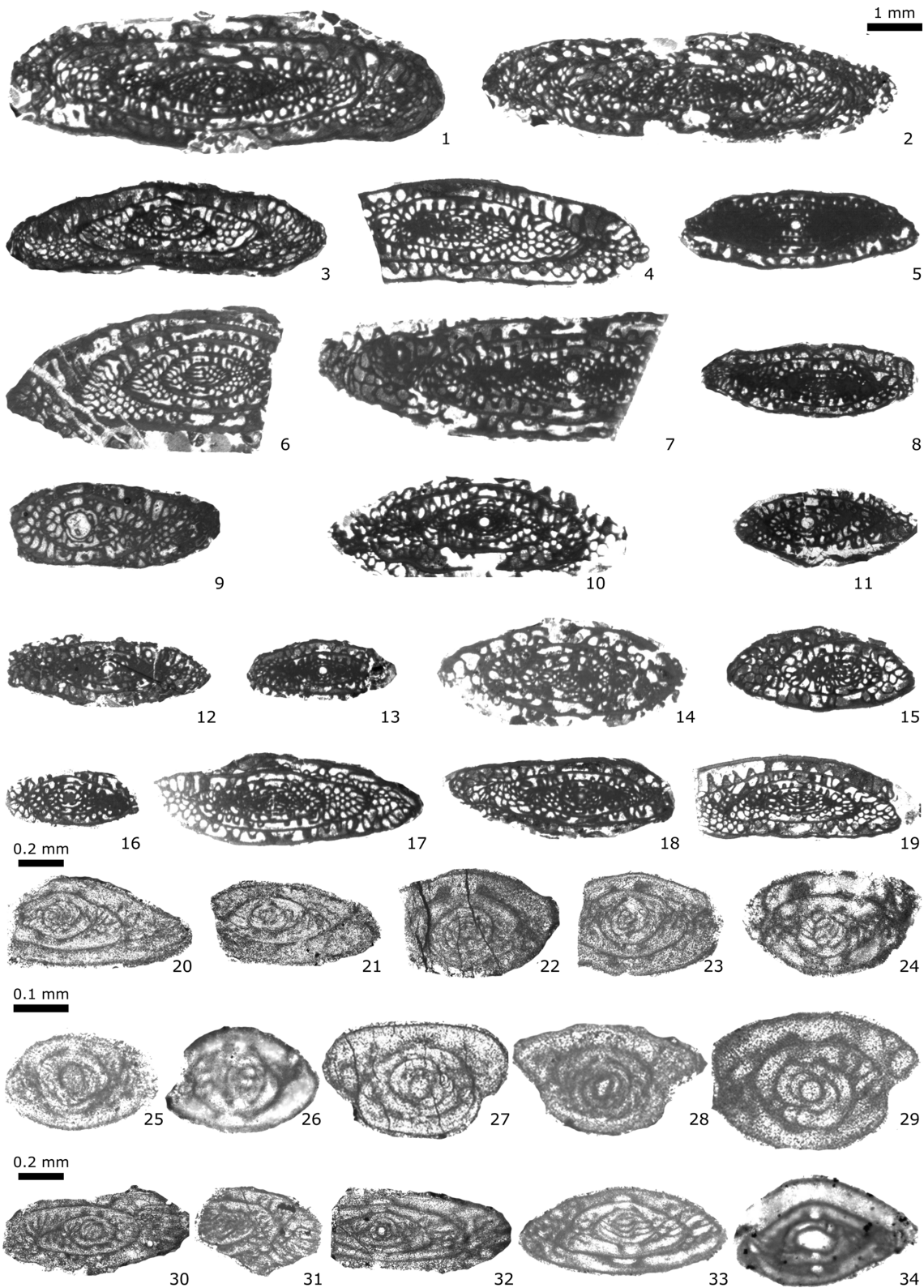
Figure 12. Fusulines from Dal'ny Tulkas trench, beds 8-1, 8-2, 10. Scale bar: 1 mm for figs 1-19; 0.2 mm for figs 20-24, 30-34; 0.1 mm for figs 25-29. 1-2. Pseudofusulina paraconcessa *Rauser, bed 8-2. 3-4.* **Pseudofusulina** *ex gr.* **pedissequa** *Vissarionovae, bed 8-2. 5.* **Pseudofusulina abortiva** *Tchuvashov, bed 8-2. 6.* **Pseudofusulina** *cf.* **utilis** *Tchuvashov, bed 8-2. 7.* **Pseudofusulina** *cf.* **salva** *Vissarionova, bed 8-2. 8, 12-13.* **Pseudofusulina seleukensis** *Rauser, bed 8-2. 9.* **Pseudofusulina** *sp. 1, bed 8-2. 10-11.* **Pseudofusulina** *ex gr.* **seleukensis** *Rauser, bed 8-2. 14-15.* **Pseudofusulina** *sp. 2, bed 8-2. 16 -19.* **Pseudofusulina urasbajevi** *Rauser, bed 8-2. 20-21.* **Schubertella** *ex gr.* **kingi** *Dunbar and Skinner, bed 8-2. 22-23.* **Schubertella** *ex gr.* **paramelonica** *Suleimanov, bed 8-2. 24.* **Schubertella** *sp. A, bed 8-2. 25-26.* **Schubertella** *aff.* **ufimica** *Baryshnikov, bed 10. 27-29.* **Schubertella** *sp. B; 27-28, bed 10; 29, bed 8-2. 30-31.* **Boultonia** *sp.; 30, bed 8-1; 31, bed 8-2. 32.* **Fusiella schubertellinoides** *Suleimanov, bed 8-1. 33.* **Mesoschubertella** *sp. 1, bed 8-2. 34.* **?Mesoschubertella** *sp. 2, bed 10.*
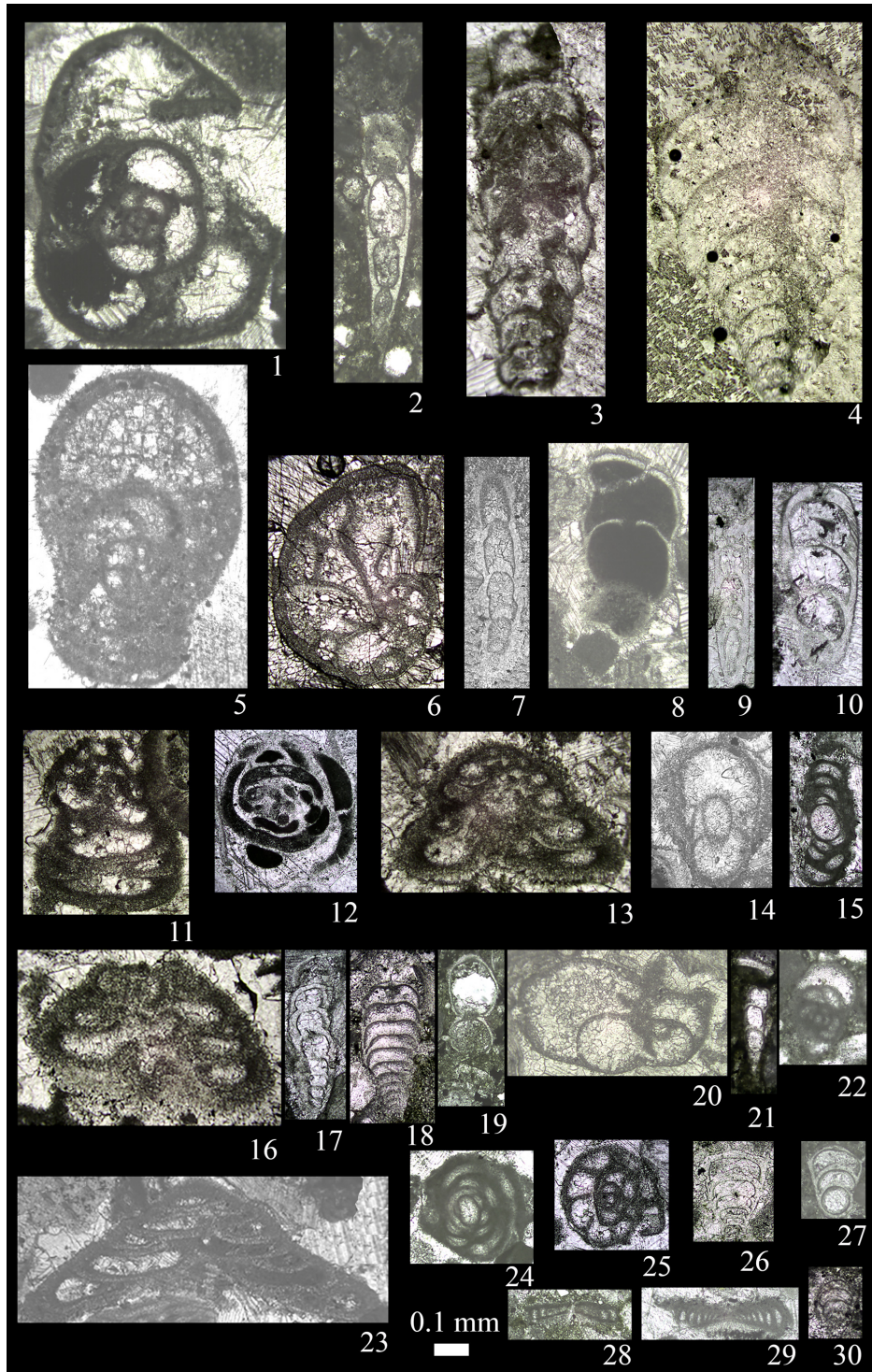
Figure 13. Small foraminiferans from the Dal'ny Tulkas trench, beds 8-1, 8-2. Scale bar: 0.1 mm. 1. **Bradyina lucida** *Morozova, bed 8-2. 2.* **Dentalina particulata** *Baryshnikov, bed 8-1. 3.* **Deckerella media bashkirica** *Morozova, bed 8-2. 4.* **Deckerella elegans multicamerata** *Zolotova, bed 8-2. 5.* **Pseudobradyina compressa** *Morozova, bed 8-2. 6.* **Globivalvulina** *sp., bed 8-2. 7.* **Dentalina particulata** *Baryshnikov, bed 8-2. 8.* **Nodosinelloides bella kamaensis** *(Baryshnikov), bed 8-2. 9.* **Nodosinelloides incelebrata novosjolovi** *Baryshnikov, bed 8-2. 10.* **Nodosinelloides netchaewi rasik** *(Baryshnikov), bed 8-2. 11.* **Tetrataxis hemisphaerica elongata** *Morozova, bed 8-2. 12.* **Pseudoagathammina dublicata** *(Lipina), bed 8-2. 13.* **Tetrataxis lata** *Spandel, bed 8-2. 14.* **Pseudobradyina compressa minima** *Morozova, bed 8-2. 15.* **Hemigordius** *sp., bed 8-2. 16.* **Tetrataxis hemisphaerica** *Morozova, bed 8-2. 17.* **Nodosinelloides jaborovensis** *Kosheleva, bed 8-2. 18.* **Geinitzina spandeli** *Tcherdynzev, bed 8-1. 19.* **Nodosinelloides kislovi** *(Koscheleva), bed 8-1. 20.* **Lateenoglobivalvulina spiralis** *(Morozova), bed 8-2. 21.* **Nodosinelloides dualis** *(Baryshnikov), bed 8-1. 22.* **Endothyra lipinae lata** *Zolotova, bed 8-1. 23.* **Tetrataxis plana** *Morozova, bed 8-2. 24.* **Hemigordiellina elegans** *(Lipina), bed 8-2. 25.* **Endothyra soshkinae** *Morozova, bed 8-2. 26.* **Geinitzina lysvaensis** *Baryshnikov, bed 8-1. 27.* **?Rectoglandulina** *sp., bed 8-1. 28.* **Postmonotaxinoides costiferus** *(Lipina), bed 8-1. 29.* **Postmonotaxinoides costiferus** *(Lipina), bed 8-2. 30.* **Howchinella** *aff. turae (Baryshnikov), bed 8-1.*

Sakmarian species as *Pseudofusulina callosa* Rauser, *P. callosa pro-concavutas* Rauser, *P. jaroslavkensis fraudulenta* Kireeva, *P.* cf. *para-jaroslavkensis* Kireeva, and *P. blochini* Korzhenevski.

A reworked assemblage of Sakmarian (Sterlitamakian) fusulines was found in a limestone which contains Artinskian conodonts: *P.* aff. *longa* Kireeva, *P. fortissima* Kireeva, *P. anostiata* Kireeva, *P. plicatissima* Rauser, *P. urdalensis abnormis* Rauser. Artinskian (Burtsevian) fusulines are found in carbonate mud matrix, including *P. callosa*, *P. plicatissima*, *P. plicatissima irregularis* Rauser, *P. urdalensis* Rauser, *P. fortissima*, *P. concavutas* Vissarionova, *P. juresanensis* Rauser, *P. consobrina* Rauser, and *P. paraconcessa* Rauser (Chernykh et al., 2015) (Table 1).

Dal'ny Tulkas trench

A new excavation was carried out in 2016 for resampling of geochemical and paleontologic characteristics. Fusulines and small foraminiferans occur in limestones at four levels. Fusulines are illustrated in figure 12 and small foraminiferans are illustrated in figures 13 and 14; both are listed in Table 1.

Three assemblages are distinguished in the trench. The first assemblage (bed 8-1) consists of 4 species of fusulines and 11 species of small foraminiferans. Species of *Boultonia*, *Schubertella*, and *Pseudofusulina* are characteristic for the Sakmarian and the Artinskian. *Fusiella schubertellinoides* Suleimanov is typical for the upper Asselian-Sakmarian. Most small foraminiferan species are Burtsevian (lower substage of Artinskian) and include *Dentalina particulata* Baryshnikov, *Geinitzina lysvaensis* Baryshnikov, *Nodosinelloides kislovi* (Koscheleva), *N. dualis* (Baryshnikov), *Howchinella* aff. *turae* (Baryshnikov), ?*Rectoglandulina* sp., *Postmonotaxinoides costiferus* (Lipina), *Endothyra lipinae lata* Zolotova. Nodosariida is predominant among them. There are *Rectoglandulina* and *Howchinella*, which appear at the base of the Burtsevian (Baryshnikov et al., 1982).

The second assemblage (bed 8-2) consists of species of 5 genera of fusulines including *Boultonia*, *Schubertella*, *Pseudofusulina*, *Fusiella* and *Mesoschubertella*. Fusulines include the frequent and varied Schubertellida, which are characteristic for the Sakmarian and Artinskian. *Pseudofusulina paraconcessa*, *Ps*. ex gr. *pedissequa* Vissarionova, *Ps. abortiva* Tchuvashov, *Ps. seleukensis* Rauser, and *Ps. urasbajevi* Rauser are characteristic of the Artinskian. Among the 32 small foraminiferan species of the second assemblage, in addition to the species from the first assemblage, there are *Langella*, and Artinskian species including *Nodosinelloides bella kamaenis* (Baryshnikov), *N. jaborovensis* (Koscheleva), *N. incelebrata novosjolovi* (Baryshnikov), *Nodosinelloides netchaewi rasik* (Baryshnikov), *Endothyra soshkinae* Morozova, numerous *Postmonotaxinoides costiferus* (Lipina), *Bradyina* ex gr. *lucida* Morozova, *Br. lucida* Morozova, *Pseudobradyina compressa* Morozova, *Deckerella elegans multicamerata* Zolotova, *Hemigordiellina elegans* (Lipina), and the first *Hemigordius* sp. The Artinskian small foraminiferan assemblages in the Urals are distinguished by the appearance of *Hemigordius*. The second assemblage also contains *Deckerella media bashkirica* Morozova, *D. elegans* Morozova, *Pseudobradyina compresa minima* Morozova, *Tetrataxis* ex gr. *conica* Ehrenberg, *T. plana* Morozova, *T. hemisphaerica* Morozova, *T. hemisphaerica elongata* Morozova, *T. lata* Spandel, characteristic of Sakmarian assemblages, and *Lateenoglobivalvulina spira-*

lis (Morozova), *Trepeilopsis* sp., and others of Cisuralian assemblages.

The third assemblage (bed 10) consists of fusulines including *Schubertella* aff. *ufimica* Baryshnikov, ?*Uralofusulinella* sp. 2. Twenty-two small foraminiferan species from the first and the second assemblages have been found in the third assemblage, and 15 species of small foraminiferans appeared for the first time in the trench. These are Burtsevian-Irginian species including *Bradyina subtrigonalis* Baryshnikov, *Endothyranella protracta maxima* Baryshnikov, *Tetrataxis lata novosjolovi* Baryshnikov, *Uralogordius* sp., *Pachyphloia* sp., *Geinitzina richteri kasib* Koscheleva, *Nodosinelloides* ex gr. *netchaewi* (Tcherdynzev), *N. jazvae* Kosheleva and Cisuralian species - *Endothyra rotundata* Morozova, *E. symmetrica* Morozova, *E. lipinae* Morozova, *Pseudoagathammina regularis* (Lipina), *Pseudospira* cf. *vulgaris* (Lipina), and the upper Artinskian-lower Kungurian *Midiella ovatus minima* (Grozdilova).

These three small foraminiferan assemblages are similar in composition to early Yakhtashian assemblages from Turkey and northern Pamir (Filimonova, 2010). The first fusuline assemblage is of Sakmarian age, the second and third are Artinskian. Typical Artinskian associations replace the schubertellid-fusuline foraminiferan associations of late Asselian-Sakmarian age. Artinskian forms of foraminiferan communities are present throughout the entire boundary interval. Their diversity and abundance increase up section.

Palynology

The palynological succession of the beds above and below the proposed Artinskian GSSP at Dal'ny Tulkas was established in the natural exposure of the section and in the excavated trench (Fig. 2). Palynological data have been gathered from both sections; the first by Michael Stephenson and the second by M.V. Oshurkova (Chernyk pers. comm. 2021).

Dal'ny Tulkas section

Materials for study comprise samples collected by Michael Stephenson between June 25 and July 4, 2007 (Stephenson, 2007). Samples (mass <200 g) were collected and processed using standard techniques (Wood et al., 1996) at the palynological laboratories of the British Geological Survey. The section sampled is shown in (Fig. 3) and consists of carbonate mudstone, siltstone and thin limestone.

The eleven samples yielded large amounts of organic residue including palynomorphs, sheet cellular material, woody material and amorphous organic matter. Palynomorphs were common in several samples, but were universally poorly preserved, showing signs of contemporaneous oxidation such that spore and pollen exine was near colourless and transparent in some cases. Saccate pollen was particularly poorly preserved with sacci commonly separated from corpi. The poor preservation necessitated staining with Safranin O to improve possibility of determination.

The most diverse and best preserved of the samples are MPA 56664, 56659, 56663, 56666 and 56662 (Fig. 15, 16). This sample range spans the proposed GSSP, which is within Bed 4 (Fig. 3).

Overall the samples are dominated by indeterminate non-taeniate and taeniate bisaccate pollen (often detached corpi or sacci), *Cycadopites* (mainly *C. glaber* (Luber and Valts) Hart) and *Vittatina* spp.
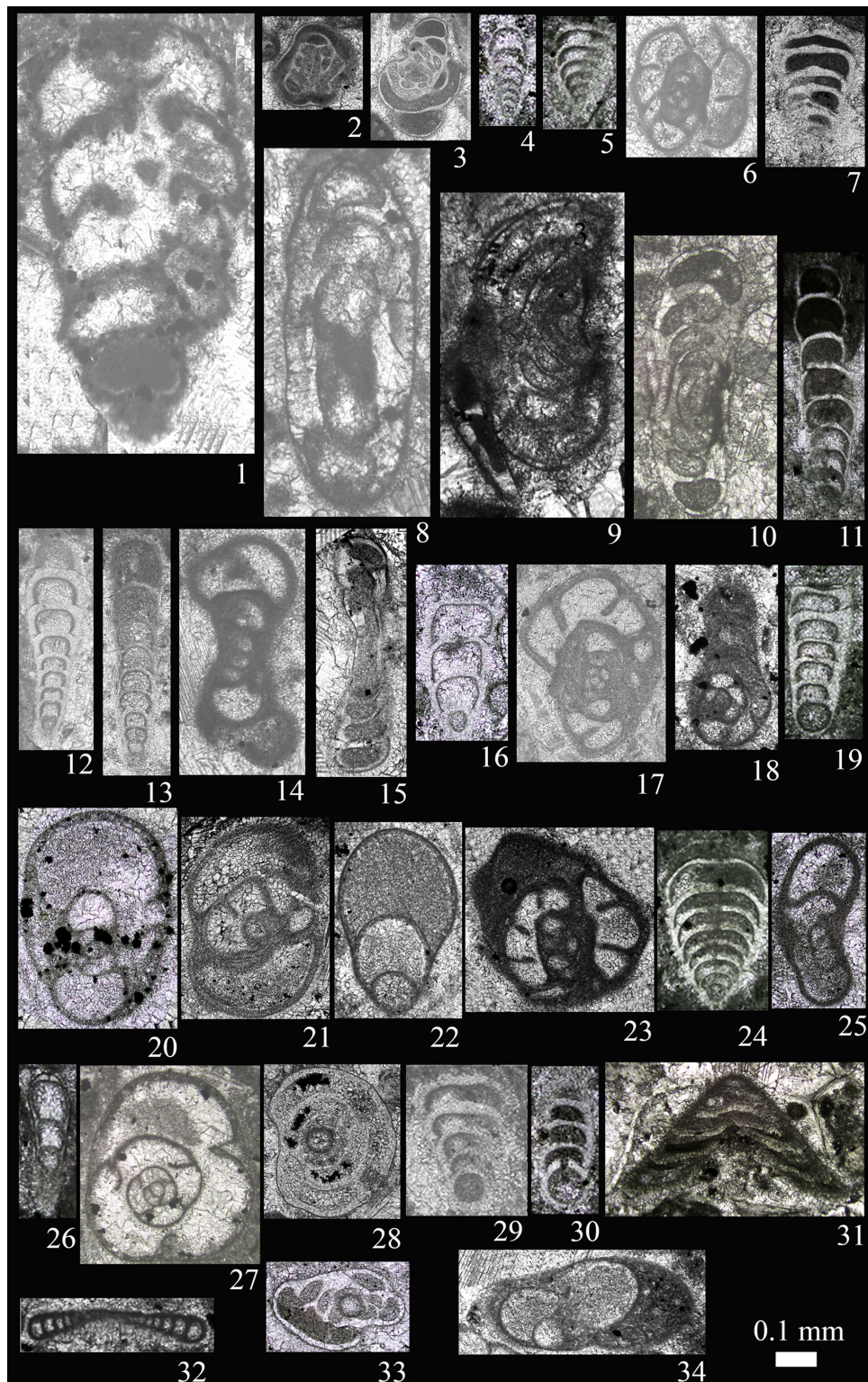
Figure 14. *Small foraminiferans from the Dal'ny Tulkas trench, bed 10. Scale bar: 0.1 mm. 1. Deckerella media bashkirica Morozova. 2. Hemigordiellina elegans (Lipina). 3. Pseudoagathammina dublicata (Lipina). 4. Howchinella aff. turae (Baryshnikov). 5. Geinitzina postcarbonica Spandel. 6. Endothyra rotundata Morozova. 7. Geinitzina richteri kasib Koscheleva. 8-10. ?Uralogordius sp. 11. Nodosinelloides bella kamaensis (Baryshnikov). 12. Nodosinelloides netchaewi (Tcherdynzev). 13. Nodosinelloides jaborovensis Kosheleva. 14. Endothyra symmetrica Morozova. 15. Hemigordius sp. 16. Nodosinelloides netchaewi rasik (Baryshnikov). 17. Endothyra soshkinae Morozova. 18. Endothyranella protracta maxima Baryshnikov. 19. Geinitzina lysvaensis Baryshnikov. 20. Pseudobradyina compressa Morozova. 21. Endothyra lipinae lata Zolotova. 22. Lateenoglobivalvulina spiralis (Morozova). 23. Endothyra rotundata Morozova. 24. Pachyphloia sp. 25. Pseudobradyina compressa minima Morozova. 26. Nodosinelloides dualis (Baryshnikov). 27. Bradyina subtrigonalis Baryshnikov. 28. Midiella ovatus minima (Grozdilova). 29. Geinitzina richteri kasib Koscheleva. 30. ?Langella sp. 31. Tetrataxis lata novosjolovi Baryshnikov. 32. Postmonotaxinoides costiferus (Lipina). 33. Pseudospira cf. vulgaris (Lipina). 34. Lateenoglobivalvulina spiralis (Morozova).*
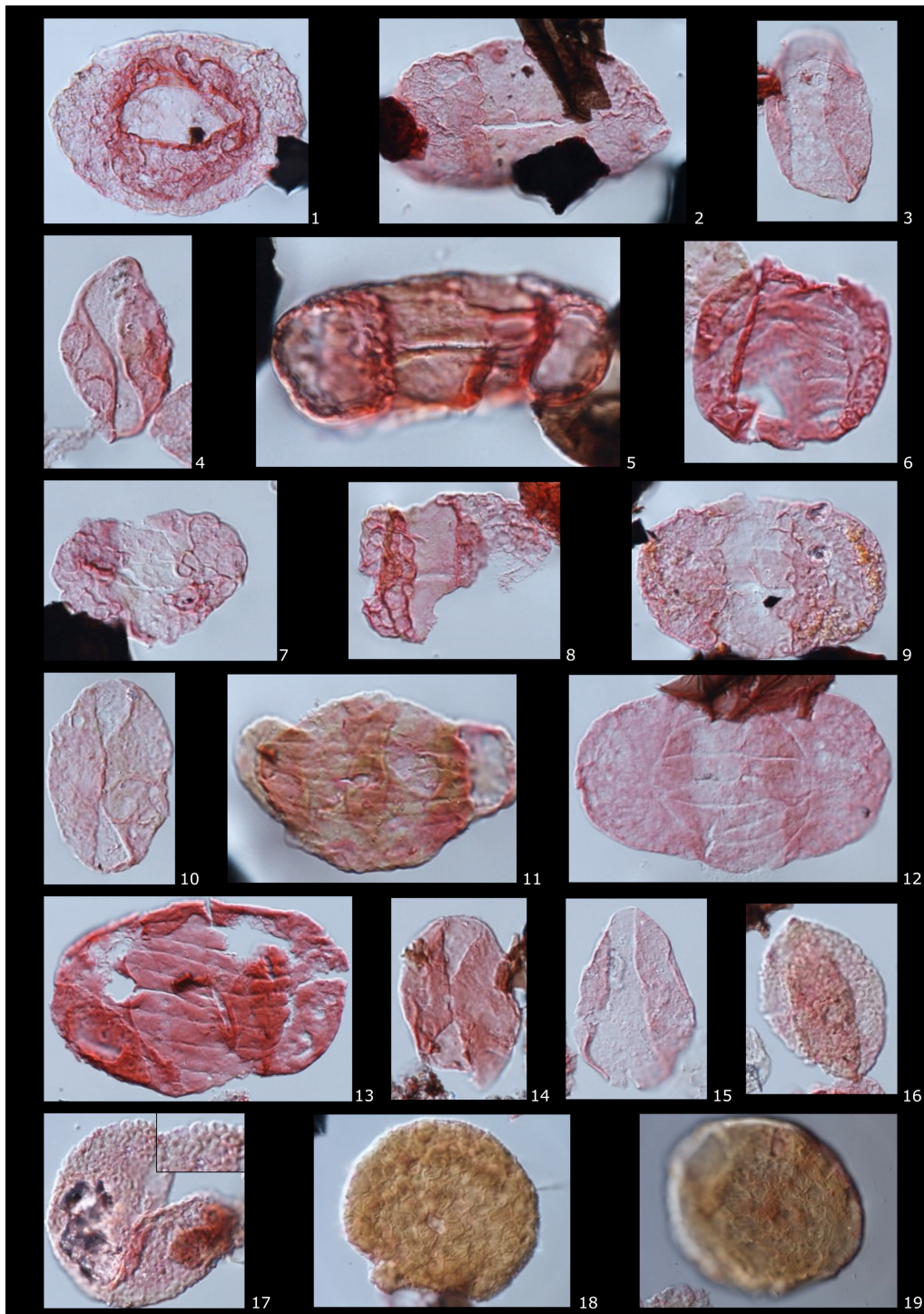
Figure 15. Palynomorphs from the Dal'ny Tulkas natural exposure section. Slides are held in the collection of the BGS, Keyworth, Nottingham, NG12 5GG, UK. Locations of specimens are given first by England Finder code, then by BGS collections numbers. (MPA, MPK). The maximum dimension of each specimen is given in microns. 1. Potonieisporites grandis *Tshudy and Kosanke 1966, E44, MPA 56666, MPK 13629, 110 µm.* **2.** Limitsporites monstruosus *Luber and Valts, F68/4, MPA 56666, MPK 13630, 95 µm.* **3.** Cycadopites ?glaber *(Luber and Valts) Hart, E47, MPA 56666, MPK 13631 50 µm.* **4.** Cycadopites ?glaber, *M57, MPA 56666, MPK 13632, 30 µm.* **5.** Limitsporites monstruosus, *D52/2, MPA 56666, MPK 13633, 55 µm.* **6.** Vittatina subsaccata *Samoilovich, D52/1, MPA 56666, MPK 13634, 45 µm.* **7.** Alisporites indarraensis *Segroves, D56/4, MPA 56666, MPK 13635, 50 µm.* **8.** Limitsporites monstruosus, *D52, MPA 56666, MPK 13636, 60 µm.* **9.** Protohaploxypinus *sp., S67, MPA 56666, MPK 13637, 65 µm.* **10.** Cycadopites ?glaber, *O60/1, MPA 56666, MPK 13638, 40 µm.* **11.** Hamiapollenites bullaeformis *(Samoilovich) Jansonius, N63/3, MPA 56666, MPK 13639, 65 µm.* **12.** ?Complexisporites *sp. O61/4, MPA 56666, MPK 13640, 80 µm.* **13.** Protohaploxypinus *sp., L59/3, MPA 56659, MPK 13641, 90 µm.* **14.** Cycadopites ?glaber, *O60/1, MPA 56659, MPK 13642, 40 µm.* **15.** Cycadopites ?glaber, *O52/2, MPA 56659, MPK 13643, 40 µm.* **16.** Algal palynomorph sp. A, *M46/2, MPA 56659, MPK 13644, 60 µm.* **17.** Algal palynomorph sp. A, *O61/3, MPA 56659, MPK 13645, 60 µm (inset detail of ornament).* **18.** Azonaletes *cf.* compactus *Luber, F51, MPA 56659, MPK 13646, 95 µm.* **19.** Azonaletes *cf.* compactus, *G57, MPA 56664, MPK 13647, 95 µm.*

(mainly *V. minima* Jansonius, *V. vittifera* (Luber and Valts) Samoilovich and *V. subsaccata* Samoilovich). Algal forms such as *Azonaletes* cf. *compactus* Luber and 'Algal palynomorph sp. A' (see Stephenson, 2007) are also locally common. Other taxa recorded include *Complexisporites* sp., *Alisporites indarraensis* Segroves, *Cordaitina* spp. (including *C. uralensis* (Luber and Valts) Samoilovich), *Crucisaccites ornatus* (Samoilovich) Dibner, *Florinites luberae* Samoilovich, *Hamiapollenites bullaeformis* (Samoilovich) Jansonius, indeterminate monosaccate pollen, *Knoxisporites* sp., *Limitsporites elongatus* Lele and Karim, *L. monstruosus* Luber and Valts, *Maculatasporites* sp., *Potonieisporites grandis* Tshudy and Kosanke, *Protohaploxypinus* spp., *Punctatisporites* sp. and *Sulcatisporites* spp. (Fig. 15).

'Algal palynomorph sp. A' is non-haptotypic and has a distinctive ornament of ring-like elements (Fig. 15). In the three lower samples, large algal palynomorphs (mean diameter approx. 100 μm) with an indistinct reticulate surface are very common, and are particularly conspicuous in slides because they do not absorb the Safranin O stain, remaining a translucent lemon yellow colour. For the present they are assigned to *Azonaletes* cf. *compactus*.

The lower part of the succession from beds 1, 2 and 3 appear to be dominated by probable algal palynomorphs such as *Azonaletes* cf. *compactus*, though indeterminate bisaccate pollen are common, including taeniate indeterminate bisaccate pollen, as well as species of *Vittatina* are present.

Beds 7 to 9 contain very few algal palynomoprhs such as *Azonaletes* cf. *compactus*, and *Cycadopites* [mainly *C. glaber* (Luber and Valts)

Hart] become more common above the proposed boundary level as do species of *Vittatina*.

Dal'ny Tulkas trench

From beds 1 to 3 in the trench (Fig. 5), M.V. Oshurkova reported common pollen such as *Vestigisporites* sp. *Hamiapollenites* sp., *Protohaploxypinus* sp., *Striatopodocarpites spp.* and *Vittatina vittifer*. Spores such as *Crassispora* sp., *Apiculatisporis* sp. and *Anaplanisporites* sp. are also present.

In beds 5 and 6, *Hamiapollenites* sp., *Protohaploxypinus* sp., and *Vittatina* spp. are again common in the trench.

Beds 7 to 9 contain *Crassispora* sp., *Cordaitina* spp. (including *C. rotata*), *Florinites luberae*, *Hamiapollenites* spp. (including *H. bullaeformis*), *Protohaploxypinus* sp., *Striatopodocarpites* spp., and *Vittatina* spp. (including *V. vittifer* and *V. striata*). A small number of *Weylandites specimens* were also recorded.

As a general comment on palynology for correlation of the base of the Artinskian, there are no markers among the spores and pollen that would provide a correlation point for the GSSP. However the probable algal taxa *Azonaletes* cf. *compactus* appears to be very common below the proposed boundary and absent above (Fig. 16). Data on the wider stratigraphic occurrence of *Azonaletes* cf. *compactus* and its biological affinity would help to decide whether it has any value as a palynological marker for the base of the Artinskian. The abundance of this taxon, in this case, coincides with proximity to the boundary. The
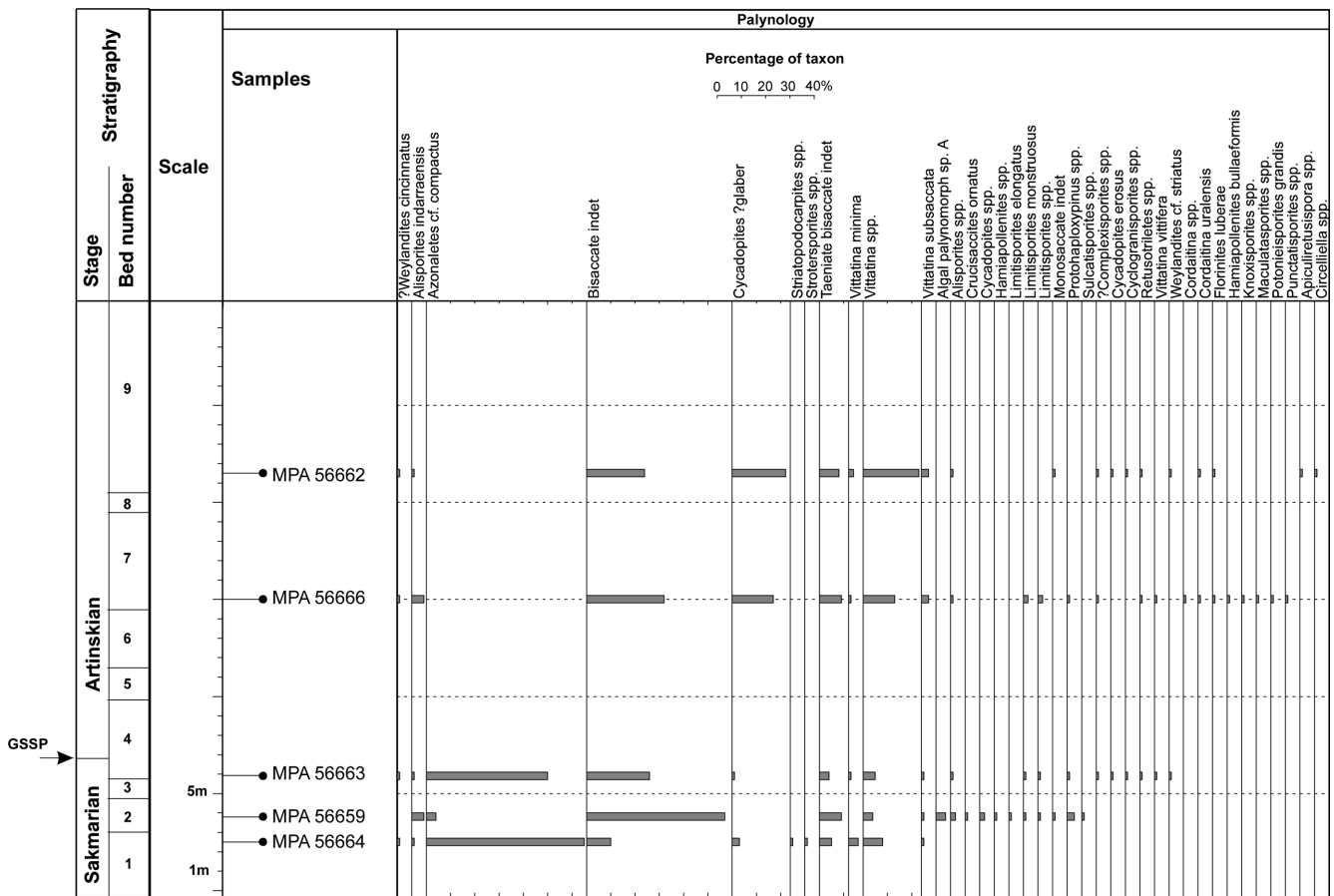
Figure 16. Simplified stratigraphic log of the Dal'ny Tulkas section showing characteristics of the palynological samples.

role of Permian palynological biostratigraphy is summarized by Stephenson (2018).

Radiolarians

Numerous radiolarians of excellent preservation, represented by 32 species (Figs. 17, 18; Table 1), occur in the sediments associated with the Sakmarian-Artinskian boundary in the trench. In this assemblage, 16 species (50%) are common with radiolarians of other assemblages of the Southern Urals (Afanasieva, 2018).

The taxonomic composition of radiolarian assemblages has been revised for the Sakmarian-Artinskian boundary interval: (1) the total number of established radiolarian species decreased; (2) the absolute and relative numbers of representatives of the class Sphaerellaria decreased; (3) the number of the species of the class Stauraxonaria decreased. However, on the other hand, the relative content of the class Spumellaria increased, and the species *Pseudoalbaillella scalprata* from the order Albaillellaria (class Aculearia) appeared.

The change in the taxonomic composition of radiolarians allows two assemblages to be established: *Tetragregnon vimineum* (lower)
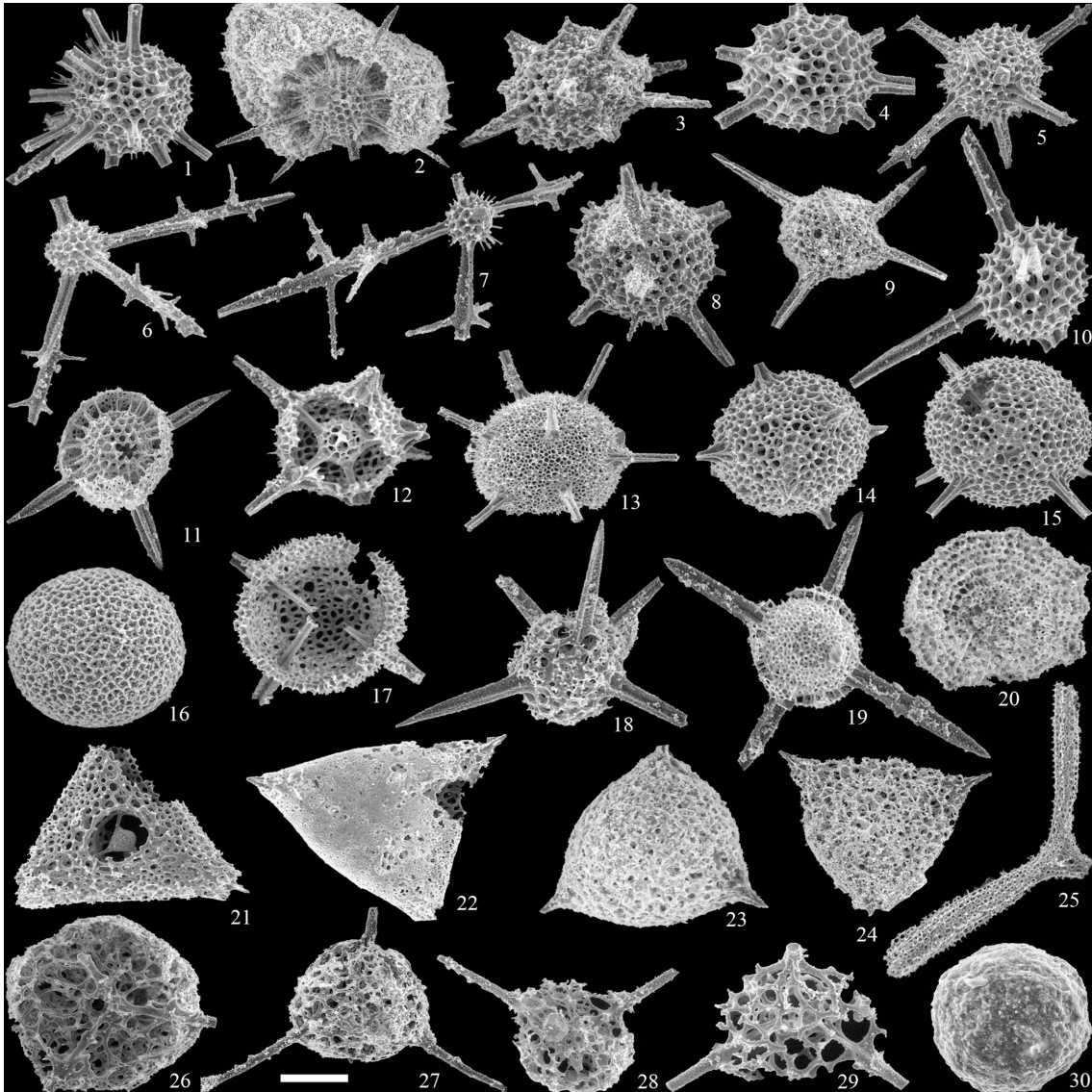
Figure 17. Radiolarians from Dal'ny Tulkas trench, bed 7-2 (figs 1–19 and 21–29) and bed 5-2 (figs 20 and 30). 1-2. **Astroentactinia** *sp. F: 1 – bar 91 µm, 2 – bar 132 µm. 3.* **A. inscita** *Nazarov in Isakova and Nazarov, bar 77 µm. 4.* **A.** *sp. G, bar 76 µm. 5.* **Apophysiacus sakmaraensis** *(Kozur and Mostler), bar 109 µm. 6-7.* **A. praepycnoclada** *(Nazarov and Ormiston): 6 – bar 92 µm, 7 – bar 91 µm. 8.* **Entactinia mariannae** *Afanasieva and Amon, bar 92 µm. 9.* **E. chernykhi** *Afanasieva and Amon, bar 95 µm. 10.* **E. dolichoacus** *Nazarov in Isakova and Nazarov, bar 63 µm. 11.* **Microporosa permica permica** *(Kozur and Mostler), bar 92 µm. 12.* **Helioentactinia** *sp. I, bar 61 µm. 13.* **H.** *sp. B, bar 139 µm. 14.* **H.** *sp. D, bar 92 µm. 15.* **H.** *sp. C, bar 110 µm. 16.* **Spongentactinia fungosa** *Nazarov, bar 69 µm. 17.* **S.** *sp. A, bar 79 µm. 18.* **S.** *sp. H, bar 86 µm. 19.* **Pluristratoentactinia** *sp. J, bar 71 µm. 20.* **Copicyntra fragilispinosa** *Kozur and Mostler, bar 91 µm. 21.* **Kozurispongus laqueus** *(Nazarov and Ormiston), bar 109 µm. 22.* **Latentidiota promiscua** *(Nazarov and Ormiston), bar 108 µm. 23.* **Nazarovispongus aequilateralis** *(Nazarov in Isakova and Nazarov), bar 68 µm. 24.* **N. pavlovi** *Kozur, bar 137 µm. 25.* **Latentifistula heteroextrema** *Nazarov in Isakova and Nazarov, bar 141 µm. 26-27.* **Tetragregnon sphaericus** *Nazarov in Isakova and Nazarov: 26 – bar 109 µm, 27 – bar 137 µm. 28-29.* **T. vimineum** *Amon, Braun and Chuvashov: 28 – bar 135 µm, 29 – bar 91 µm. 30.* **Palaeodiscaleksus** *cf.* **punctus** *(Hinde), bar 80 µm.*

and *Pseudoalbaillella scalprata* (upper). The quantitative ratio of taxa of higher rank (classes) reflects the characteristic of each assemblage.

Tetragregnon vimineum Assemblage

The terminal Sakmarian radiolarian assemblage is represented by 26 species (Figs. 17): Sphaerellaria – 13 species (50%), Spumellaria – five species (19.2%), Stauraxonaria – eight species (30.8%). Among the radiolarians of this assemblage, 13 species are found only in the Sakmarian Stage. The association of radiolarians from the trench is

considered characteristic of the *Tetragregnon vimineum* Assemblage within the range of the *Sweetognathus anceps* conodont zone.

Pseudoalbaillella scalprata Assemblage

The basal Artinskian radiolarian assemblage is represented by 19 species (Figs. 18): Sphaerellaria – nine species (47.4%), Spumellaria – five species (26.3%), Stauraxonaria – four species (21%), the bilaterally symmetrical species *Pseudoalbaillella scalprata* appears. Among the radiolarians of this assemblage, six species are characteristic only
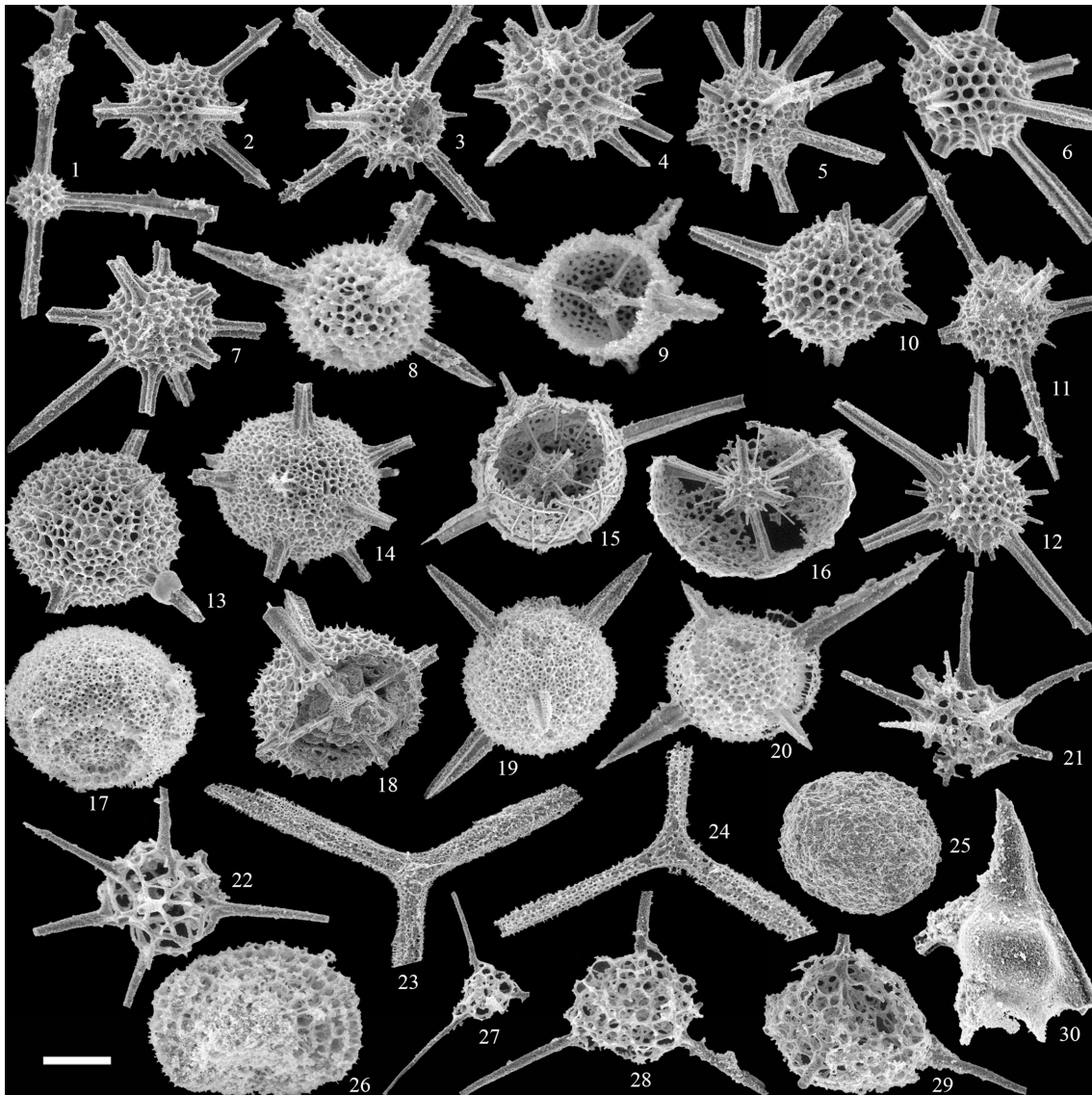
Figure 18. Radiolarians from Dal'ny Tulkas trench, bed 10-1 (figs 2, 3, 5, 7, 11–14, 18, 19, and 23), bed 11-2 (figs 1, 4, 6, 8–10, 15, 16, 20-22, and 24–30), and bed 11-3 (fig. 17). 1. Apophysiacus praepycnoclada *(Nazarov and Ormiston), bar 90 μm.* **2-3.** A. sakmaraensis *(Kozur and Mostler): 2 – bar 109 μm, 3 – bar 91 μm.* **4.** Astroentactinia inscita *Nazarov in Isakova and Nazarov, bar 77 μm.* **5–7.** A. sp. G: *5 – 94 μm, 6 – 68 μm, 7 – 91 μm.* **8–10.** Bientactinosphaera *sp. E: 8 – 59 μm, 9 – 49 μm, 10 – 69 μm.* **11-12.** Entactinia dolichoacus *Nazarov in Isakova and Nazarov: 11 – bar 109 μm, 12 – bar 95 μm.* **13.** Helioentactinia *sp. C, bar 103 μm.* **14.** H. *sp. B, bar 120 μm.* **15-16.** Paratriposphaera strangulata *(Nazarov and Ormiston): 15 – bar 113 μm, 16 – bar 91 μm.* **17.** Copicyntra fragilispinosa *Kozur and Mostler, bar 71 μm.* **18.** Spongentactinia *sp. A, bar 117 μm.* **19.** Pluristratoentactinia lusikae *Afanasieva, bar 89 μm.* **20.** P. *sp. J, bar 52 μm.* **21-22.** Secuicollacta amoenitas *Nazarov and Ormiston, bar 76 μm.* **23-24.** Latentifistula heteroextrema *Nazarov in Isakova and Nazarov: 23 – bar 220 μm, 24 – bar 166 μm.* **25.** Palaeodiscaleksus *cf.* punctus *(Hinde), bar 135 μm.* **26.** Rectotormentum fornicatum *Nazarov and Ormiston, bar 60 μm.* **27–29.** Tetragregnon vimineum *Amon, Braun and Chuvashov, possible successive stages of skeleton formation, bar 122 μm.* **30.** Pseudoalbaillella scalprata *Holdsworth and Jones, bar 69 μm.*

of the Artinskian Stage.

Bilaterally symmetrical radiolarians from the order Albaillellaria are of special note because they are extremely rare in the Southern Urals. *Pseudoalbaillella scalprata* was first described from the Lower Permian, Leonardian (late Artinskian-Kungurian) deposits of the Havallah Formation in Nevada, USA (Holdsworth and Jones, 1980). Later, Murchey (in Stewart et al., 1986) noted that *P. scalprata* was found in the same sample with the conodont *Mesogondolella idahoensis*, the presence of which indicates a late Kungurian age (Lambert et al. 2007; Henderson et al., 2012; Wardlaw and Nestell, 2015; Nestell and Nestell, 2020).

The skeleton of *Pseudoalbaillella scalprata* is distinguished by a very short pseudoabdomen (25 µm), a wide conical apical cone and a wingspan of 70° (Holdsworth and Jones, 1980, fig. 1A). The specimen of *Ps. scalprata* found in the trench is characterized by the same parameters of the skeleton and a wingspan of 75°.

The species *Pseudoalbaillella scalprata* is very loosely interpreted by different researchers, both in terms of morphological features and age. The discovery of the species *Pseudoalbaillella scalprata* in the trench confirms the morphological features of this species (Holdsworth and Jones, 1980, fig. 1A), and clarifies the boundaries of its biostratigraphic distribution from the base of the Artinskian to the Kungurian.

The association of radiolarians from the trench is considered as characteristic of the *Pseudoalbaillella scalprata* Assemblage within the range of the *Sweetognathus asymmetricus* conodont zone.

A recent summary of Permian radiolarian biostratigraphy is provided by Zhang et al. (2018). However, unfortunately, none of the Lower Permian radiolarian zones has been established in the Southern Urals, since representatives of the genus *Pseudoalbaillella* are extremely rare here. The first biostratigraphic scale based on lower Permian radiolarians (Nazarov and Ormiston, 1985, 1999; Nazarov, 1988) comprised ten beds with characteristic faunas. These assemblages have been recognized in the territory of the Southern Urals and Western Mugodzhary.

At present, eighteen Lower Permian radiolarian assemblages are recognized as valid based on the data for thirteen reference sections of the Greater Urals and Western Mugodzhary (Afanasieva, 2018, 2021). Two new assemblages (*Tetragregnon vimineum* and *Pseudoalbaillella scalprata*) complement the radiolarian biostratigraphic scale in the Southern Urals.

U-Pb Geochronology

Schmitz and Davydov (2012) carried out radioisotopic studies, based upon high-precision, isotope dilution-thermal ionization mass spectrometry (ID-TIMS) U-Pb zircon ages for interstratified volcanic ash beds in sections of the southern Urals, including the Dal'ny Tulkas section. Here they selected ash tuffs at three levels (see black stars for levels in Fig. 3) - in the upper part of bed 2 (4 m lower than base of Artinskian, in the upper part of bed 7 and in the base of bed 9 (2 m higher than the previous sample).

In bed 2, of eight analyzed grains of zircon, six grains yielded a weighted mean ^{206}Pb/^{238}U date of 290.81 ± 0.09 Ma. Seven of eight analyzed grains from bed 7 produced a weighted mean ^{206}Pb/^{238}U date of 288.36 ± 0.10 Ma. And from the third interlayer of ash tuff (bed 9) all eight investigated grains gave a ^{206}Pb/^{238}U date of 288.21 ± 0.06 Ma.

The three dated samples allow the calculation of a relatively constant accumulation rate through the lower portion of the section (Schmitz and Davydov, 2012, p. 561). These zircons provided an interpolated geochronometric age of 290.1 Ma ± 0.2 Myr (Schmitz and Davydov, 2012; Henderson et al., 2012) and 290.5 Ma ± 0.4 Myr (Henderson and Shen, 2020) for the base-Artinskian. The radiometric ages determined from Dal'ny Tulkas sections will be of considerable value for correlations with non-marine Permian sections.

Strontium Isotopes

Schmitz et al. (2009) in a presentation at the International Conodont Symposium indicated a consistent secular trend of ^{87}Sr/^{86}Sr isotopic ratios from conodont elements through the Lower Permian. The ^{87}Sr/^{86}Sr ratio for the base-Artinskian is based on material from Dal'ny Tulkas and from Usolka was approximately 0.70765 (Schmitz et al., 2009). Strontium isotopes from individual conodont elements can be integrated with geochronometric ages to produce a time model. The strontium isotopic composition of seawater at the base of the Artinskian Stage is now calculated at ^{87}Sr/^{86}Sr = 0.70767 (Chernykh et al., 2012); they also provided a description of the methodology used by Mark Schmitz. Only well preserved specimens with colour alteration index <2.0 were measured. One to ten elements were pooled by genera and cleaned and partially dissolved. The undissolved portion were dissolved in nitric acid and Sr separated on Sr-spec crown ether resin. Sr isotope ratios were measured by thermal ionization mass spectrometry (TIMS) with a reported reproducibility of +/- .00001. It was indicated that a smoothed spline fit to these data with 95% confidence interval yielded a chronostratigraphic proxy with a resolution of about .5 Ma. The isotopic values from conodonts provided in Chernykh et al. (2012; their fig. 8) were somewhat more radiogenic than isotopic values from brachiopods determined by Korte et al. (2006) from the same sections for the Sakmarian – lower Artinskian interval, but the reverse was true for brachiopods around the Carboniferous-Permian boundary from Usolka; this might suggest diagenetic variability. However, all of these conodonts and brachiopods were considered to not be diagenetically altered. Future analyses will need to investigate these differences in order to enhance this method as a correlation tool. A summary figure of the Sr secular trend is also depicted in fig. 24.9 in GTS 2012.

Carbon Isotope Chemostratigraphy

A group of Chinese researchers with the participation of V.I. Davydov (USA, Boise State University) conducted a study of carbon and oxygen stable isotopes in the GSSP candidate sections of the South Urals – Usolka, Dal'ny Tulkas and Kondurovsky (Zeng et al., 2012). Basic results, obtained from the Dal'ny Tulkas section are provided below.

In the Dal'ny Tulkas section the curves of δ^{13}C and δ^{18}O display a general concurrent change with a rapid drop near the Sakmarian-Artinskian boundary and a long-term depletion in the subsequent part of the Artinskian Stage (Fig. 19). The values of δ^{13}C present a dramatic depletion to approximately −16‰. However, no similar δ^{13}C excursions around the Sakmarian-Artinskian boundary have been observed in other sections, including the Naqing and Zhongdi sections in South
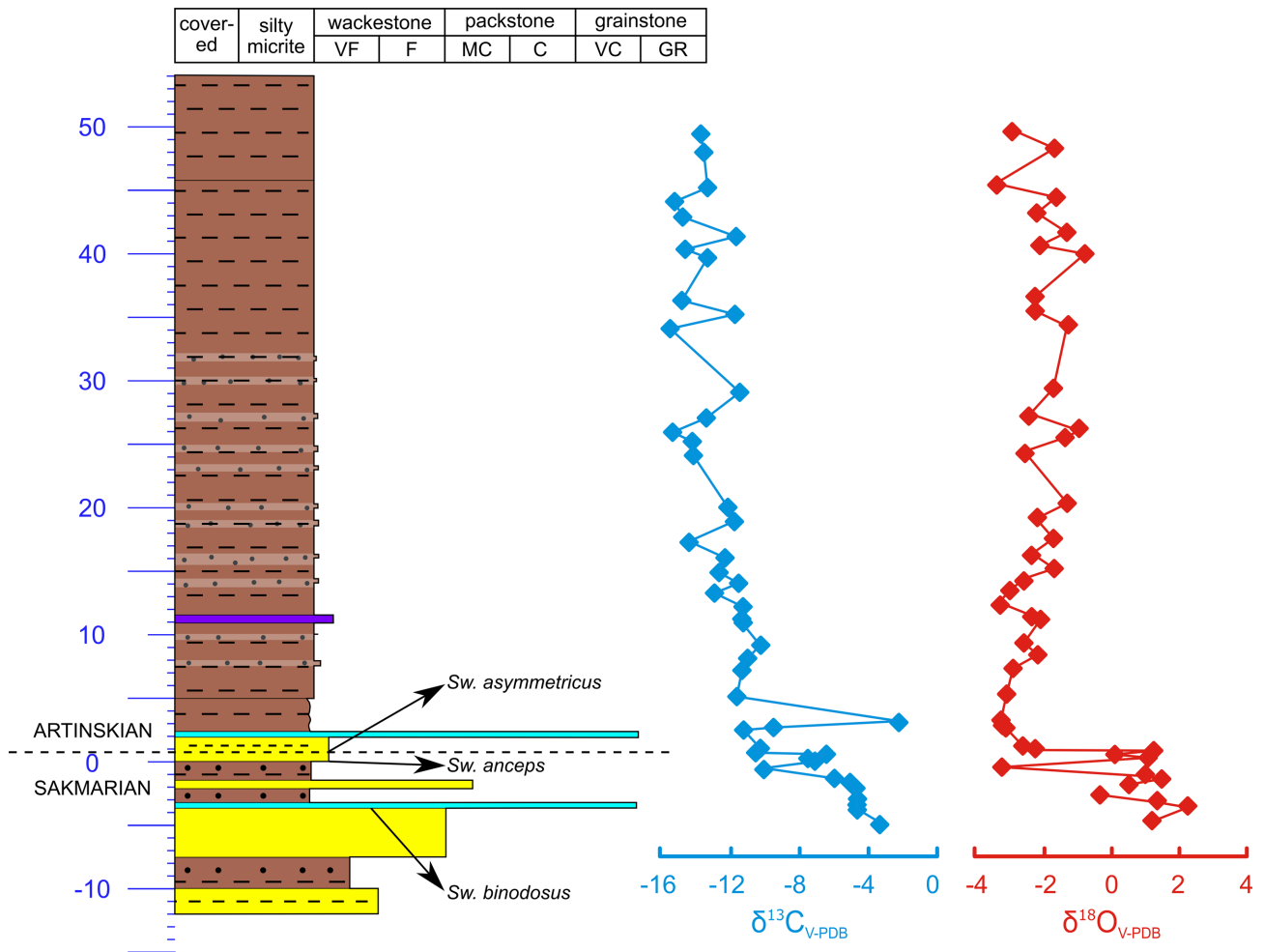
Figure 19. Carbon and oxygen isotopic composition of the Dal'ny Tulkas section (modified from Zeng et al., 2012).

China (Buggisch et al., 2011). These very negative values and concurrent trends in both carbon and oxygen isotopic compositions at Dal'ny Tulkas are attributed to diagenesis. Buggish et al. (2011) showed an increase of about 1.5‰ from the upper part of the Sakmarian to the lower part of the Artinskian in the Naqing section and of about 3‰ in the Zhongdi and Kongshan succession in China. This positive trend was not observed in Dal'ny Tulkas, but may provide the potential for correlation in other sections.

Paleomagnetic Stratigraphy

The Sakmarian-Artinskian boundary occurs within the long Kiaman superchron. Hounslow and Balabanov (2018) report a short normal polarity (C12n) within the upper Artinskian, but otherwise paleomagnetic data will not assist correlation of the boundary. This is confirmed in a paleomagnetic study of the Dal'ny Tulkas section by Balabanov et al. (2019). They demonstrate that the primary component of magnetization was well preserved, but no changes or reversals in the remanent magnetization were recognized in the boundary interval.

Gondwana Correlations

Correlation between the paleo-equatorial province in which the

Permian Stage GSSPs are based and Gondwana has been historically difficult mainly because the conodonts on which Permian Stage GSSPs are based are largely absent from Gondwana basins (comazzon et al., 2013; Stephenson, 2016; Mouro et al., 2020).

Australia has some of the best documented Permian basins in Gondwana, but most of the succession is nonmarine. Calibration of the local palynostratigraphic scheme (Price, 1997) to the global timescale was indirect and very difficult, having traditionally relied on correlations from relatively sparse, high-latitude, marine strata, where ammonoids and conodonts are rare, fusulines are unknown, and much of the other faunas (brachiopods and bivalves) are endemic. Tie points are rare and often tenuous (Mantle et al., 2010). One example is the record of a single specimen of the ammonoid *Cyclolobus persulcatus* from the Cherrabun Member of the Hardman Formation, in the Canning Basin, Western Australia (Foster and Archbold, 2001), dated as 'post-Guadalupian' by Glenister et al. (1990) and 'Capitanian–Dzhulfian' by Leonova (1998).

Recent advances in high-precision U-Pb CA-TIMS dating of Middle Permian to Lower Triassic successions in eastern Australian Gondwana have seen major advances in the ability to date lithostratigraphic units (Metcalfe et al., 2015; Nicoll et al., 2015; Bodorkos et al., 2016; Laurie et al., 2016). Based on these new dates, the Guadalupian-Lopingian (Capitanian-Wuchiapingian) boundary is tentatively
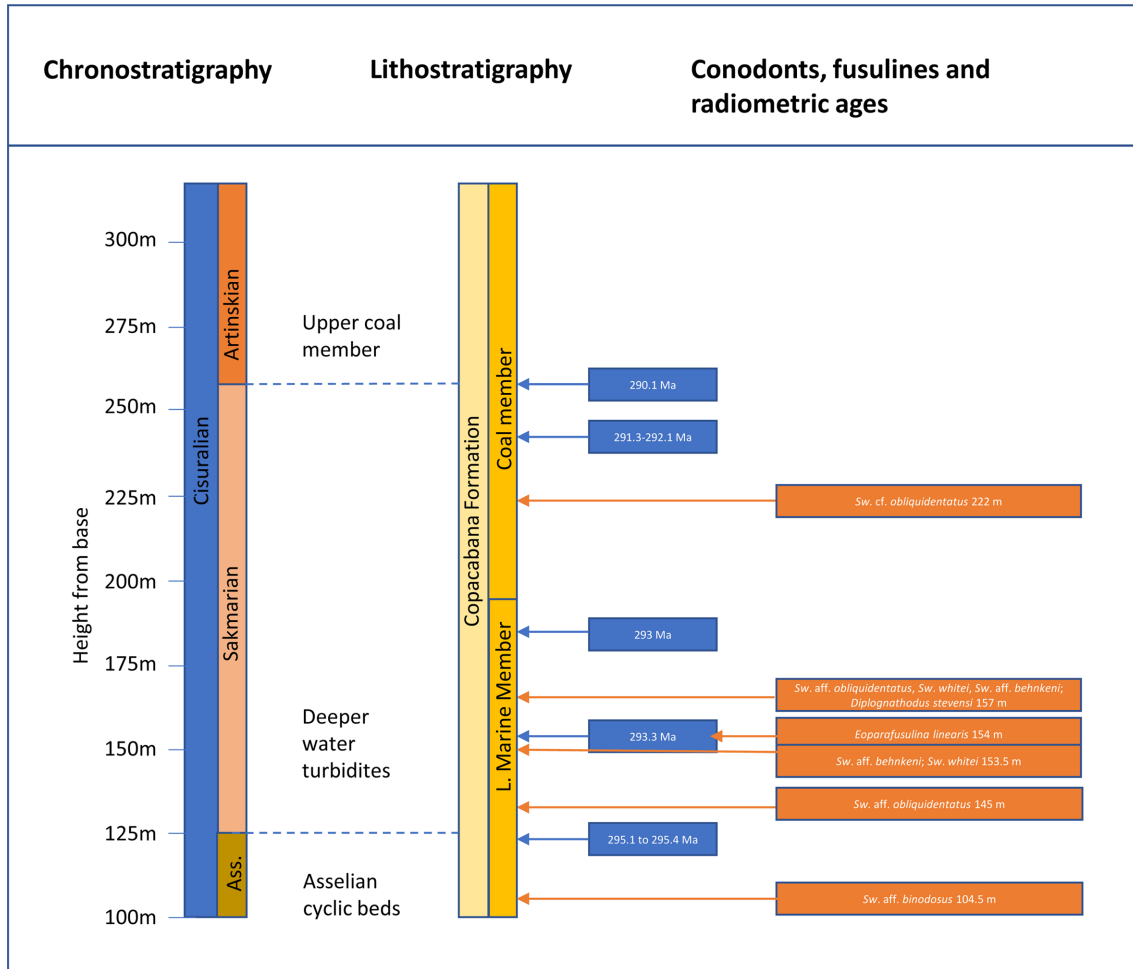
Figure 20. Summary of relevant dates and conodont occurrences from the Apillapampa section (Copacabana Formation) (modified after di Pasquo 2015). Conodonts updated from those previously reported by Henderson et al. (2009). Dashed blue lines represent sequence boundaries.

placed at the level of the Thirroul Sandstone in the lower part of the Illawarra Coal Measures in the Sydney Basin. The Wuchiapingian-Changhsingian boundary is at or close to the Kembla Sandstone horizon in the Illawarra Coal Measures, southern Sydney Basin, in the middle part of the Newcastle Coal Measures in the northern Sydney Basin, and in the middle of the Black Alley Shale in the southern Bowen Basin. However none of these dates allow the Dal'ny Tulkas Artinskian units to be correlated to Australia because the newly dated Australian units are all younger, but presumably correlative units may be found in the Pebbley Beach Formation of the Sydney Basin (Metcalfe et al., 2015) with its associated brachiopods, bivalves, plants, abundant trace fossils and dropstones.

In South America, volcanic ash beds within the Cisuralian are much more common than in other Gondwana Permian basins and dates are becoming available, particularly for the Paraná Basin in Brazil and the Tarija Basin of central Bolivia.

Dates from the Paraná Basin are now abundant (e.g., Rocha-Campos et al., 2006, 2007, 2019; Guerra Sommer et al., 2008a, b, c; Griffis et al., 2018, 2019; Santos et al., 2006; Simas et al., 2012; Jurigan et al., 2019; Cagliari et al., 2020), but vary greatly in precision. Those concentrating on the *Vittatina costabilis* palynological biozone are most relevant to the Dal'ny Tulkas section because several high precision CA-ID-TIMS radiometric dates (see Souza et al., 2021) indicate that

the zone ranges in age from the Asselian to the early Artinskian. This indicates in turn that the upper part of the Rio Bonito Formation is likely early Artinskian and similar in age to the Dal'ny Tulkas section. It should be noted that Paraná Basin rocks (Itarare Group) contain only Pennsylvanian and lowermost Asselian conodonts (Scomazzon et al., 2013; Mouro et al., 2020) so correlations can only be drawn using radioisotopic dates without the corroborating evidence of conodonts.

In this regard the Apillapampa section (Copacabana Formation) near Cochabamba, central Bolivia, is key to a more reliable correlation because it contains conodonts, fusulines and dated ash beds. Di Pasquo et al. (2015) quoted radiometric dates from six volcanic ash beds within the section; these dates were first presented in a talk by Henderson et al. (2009) based on analyses performed at Boise State University by J. Crowley and M. Schmitz. The six dates (cited as preliminary in Permian ICS Newsletter *Permophiles*, 53, Supplement 1) are 298 (40 m), 295.2 (120 m), 293.3 Ma (154 m), 293 Ma (185 m), 291.6 Ma (242 m) and 290.1 Ma (262 m) (Fig. 20). These dates are CA-ID-TIMS dates, but the precision has not been published yet. These dates fix the upper Coal Member of the Copacabana Formation as late Sakmarian to early Artinskian. The presence of the conodont *Sweetognathus* cf. *obliquidentatus* corroborates this correlation. *Sweetognathus whitei* and *Sw.* aff. *behnkeni* occur lower in the section within turbidite facies; these taxa are typical of the upper Asselian and

lower Sakmarian (Henderson, 2018; Petryshen et al., 2020). These taxa are the same reported by Suarez Riglos et al. (1987) from the Yaurichambi locality of the Copacabana Formation near La Paz, but the taxonomic identifications and relative age assignments have been revised.

Conclusion

The Dal'ny Tulkas section has the following characteristics necessary to substantiate its status as the GSSP for the base-Artinskian Stage.

1. The section is easily accessible and currently has a complete paleontological record for three key Permian biostratigraphic groups of micro- and macrobiota — conodonts, ammonoids, and foraminiferans.

2. In the section, the lower boundary of the Artinskian Stage at 0.6 metres above the base of bed 4b corresponds to the first appearance of the marker species *Sweetognathus asymmetricus* Sun and Lai in the continuous phylogenetic lineage of *Sweetognathus expansus - Sw.* aff. *merrilli - Sw. binodosus - Sw. anceps - Sw. asymmetricus*.

3. The ammonoids *Neopronorites skvorzovi*, *Uraloceras involutum*, *U. gracilentum*, and *Popanoceras annae* represent markers of the Sakmarian-Artinskian boundary.

4. The foraminiferan assemblages indicate that in the Sakmarian-Artinskian boundary interval of the Dal'ny Tulkas section, the schubertel-lid-fusuline assemblages of late Asselian-Sakmarian age are replaced by typical Artinskian forms. In the assemblages of small foraminiferans there are Artinskian forms with wide stratigraphic distribution throughout the entire boundary interval.

5. Volcanic ash beds are present and radioisotopic ages of zircons have been interpolated between 290.1 Ma ± 0.2 Myr and 290.5 Ma ± 0.4 Myr.

6. A Sr isotopic ratio of .70767 provides additional means for correlation. Unfortunately, carbon isotopic compositions are diagenetically altered and cannot be used for correlation.

7. A paleomagnetic study showed good preservation of the remanent magnetism, but no reversals were recognized in the boundary interval.

8. Numerous additional fossil groups have also been recorded from Dal'ny Tulkas including radiolarians, acritarchs, palynomorphs, brachiopods, fishes, and plant remains (algae and calamite trunks). The large diversity of fossils makes this section very attractive for paleontologists.

9. The base-Artinskian occurs within a transgressive systems tract and close to a major maximum flooding surface. This succession occurs above cyclic deposits and coupled with detailed biostratigraphy, it forms a recognizable sequence biostratigraphic signature and strong physical stratigraphic correlation tool.

10. Davydov et al. (2007) reported in *Permophiles* 50 that government agreement has been reached to protect all of the defined and proposed Cisuralian GSSP sites. The Dal'ny Tulkas site is now included in the Toratau Geopark and in the future may become one of the educational and tourist centres in the Republic of Bashkortostan, Russia.

The Global Stratotype Section and Point

The base-Artinskian GSSP is defined at 0.6 m above the base of
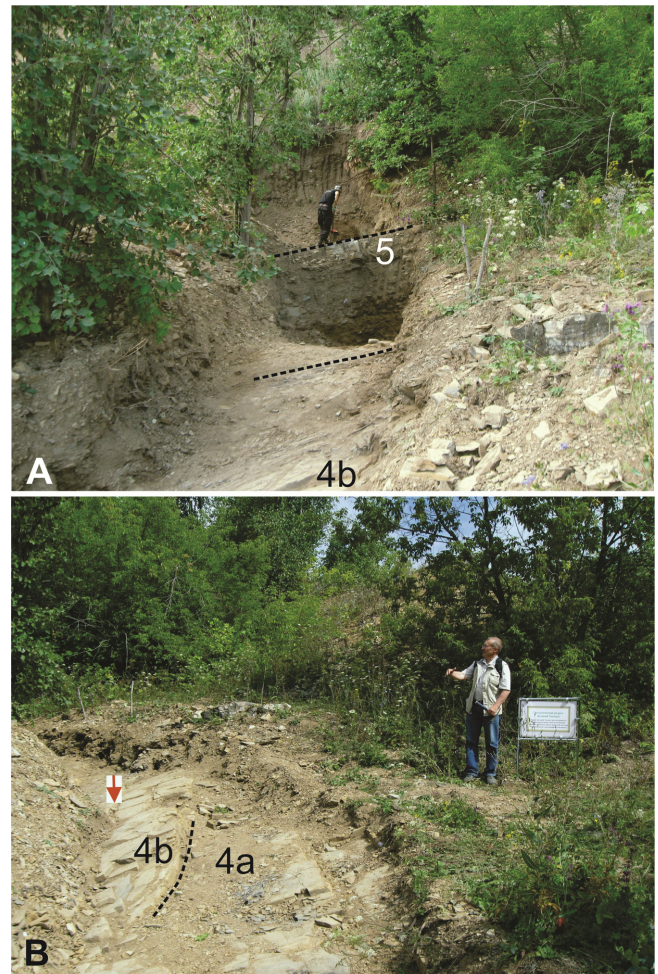
Figure 21. A. Excavated Dal'ny Tulkas section showing bed 4b and bed 5. B. Excavated Dal'ny Tulkas section at an angle and immediately below photo A, showing beds 4a and 4b with GSSP level (0.6 m above base of 4b) indicated by red arrow.

bed 4b at the Dal'ny Tulkas section (Fig. 21) in the southern Urals of Russia (53.88847N and 056.51615E). This point corresponds to the First Appearance Datum of the conodont *Sweetognathus asymmetricus*, which is part of a well defined and widely distributed lineage. Additional markers for correlation include a radioisotopic age interpolated between 290.1 and 290.5 Ma, a strontium isotopic ratio of .70767, and many additional fossils groups, particularly ammonoids and fusulines, but also small foraminiferans, radiolarians, and palynomorphs. Finally, the boundary occurs within a transgressive succession, near, or at a maximum flooding surface in many sections, thereby forming a distinctive sequence stratigraphic signature in the field. A Standard Auxiliary Boundary Stratotype (SABS) at Carlin Canyon, Nevada is in development to provide open and free access to the interval from upper Asselian to mid-Artinskian (see Angiolini et al., 2023).

Acknowledgements

References

Afanasieva, M.S., 2018, Early Permian Radiolarian Eco-Zones in the Great Urals, Northern Mygodzhary and Peri-Caspian Basin. In Nurgaliev, D., Barclay, M., Nikolaeva, S., and Silantiev, V. eds. Proceedings of Kazan Golovkinsky Stratigraphic Meeting 2017, Advances in Devonian, Carboniferous et Permian Research: Stratigraphy, Environments, Climate and Resources. Filodiritto, pp. 11–18.

Afanasieva, M.S., 2021, Asselian and Sakmarian (Lower Permian) Radiolarian Ecozones in the South Urals, Russia. Paleontological Journal, v. 55, pp. 825–862.

Angiolini, L., Beauchamp, B., Bratton, L., Fraser, B., Henderson, C.M., Snyder, W.S., and Zanchi, A., 2023, The Once and Future Quest: the Kungurian GSSP candidate at Rockland Section and SABS at Carlin Canyon, Nevada. Permophiles, 74, pp. 37–41.

Balabanov, Y.P., Sungatullin, R.Kh., Sungatullina, G.M., Kosareva, L.R., Glukhov, M.S., Yakunina, P.G., Zhernenkov, A.O., Antonenko, V.V., and Churbanov, A.A., 2019, Magnetostratigraphy of the Reference Sections of the Cisuralian Series (Permian System). In Nurgaliev D. et al. (eds.), Recent Advances in Rock Magnetism, Environmental Magnetism and Paleomagnetism, Springer Geophysics, pp. 317–342. Springer International Publishing AG, part of Springer Nature 2019. doi:10.1007/978-3-319-90437-5_23

Baryshnikov, V.V., Zolotova, V.P., and Kosheleva, V.F., 1982, Novye vidy foraminifer artinskogo yarusa Permskogo Priuralia [New Species of Artinskian Foraminifers from the Permian Cis-Urals] Preprint No., UNTs AN SSSR, Sverdlovsk, 54 p. (in Russian)

Beauchamp, B., and Henderson, C.M., 1994, The Lower Permian Raanes, Great Bear Cape and Trappers Cove formations, Sverdrup Basin, Canadian Arctic: stratigraphy and conodont zonation. Bulletin of Canadian Petroleum Geology, v. 42, pp. 562–597.

Beauchamp, B., Calvo Gonzalez, D., Henderson, C.M., Baranova, D.V., Wang, H.Y., and Pelletier, E., 2022a, Late Pennsylvanian–Early Permian tectonically-driven stratigraphic sequences and carbonate sedimentation along northern margin of Sverdrup Basin (Otto Fiord Depression), Arctic Canada. In Henderson, C.M., Ritter, S., and Snyder, W.S. eds. Late Paleozoic and Early Mesozoic Tectonostratigraphy and Biostratigraphy of western Pangea. SEPM Special Publication 113, pp. 226–254. doi:10.2110/sepmsp.113.12

Beauchamp, B., Henderson, C.M., Dehari, E., Waldbott von Bassenheim, D., Elliot, S., and Calvo Gonzalez, D. 2022b, Carbonate sedimentology and conodont biostratigraphy of Late Pennsylvanian-Early Permian stratigraphic sequences, Carlin Canyon, Nevada: new insights into the tectonic and oceanographic significance of an iconic succession of the Basin and Range. In Henderson, C.M., Ritter, S., and Snyder, W.S. eds. Late Paleozoic and Early Mesozoic Tectonostratigraphy and Biostratigraphy of western Pangea. SEPM Special Publication 113, pp. 34–71. doi:10.2110/sepmsp.113.14

Boardman, D.R., Wardlaw, B.R., and Nestell, M.K., 2009, Stratigraphy and conodont biostratigraphy of uppermost Carboniferous and Lower Permian from North American Midcontinent. Kansas Geological Survey Bulletin, v. 255, pp. 253.

Bodorkos, S., Crowley, J., Holmes, E., Laurie, J., Mantle, D., McKellar, J., Mory, A., Nicoll, R., Phillips, L., Smith, T., Stephenson, M.H., and Wood, G., 2016, New dates for Permian palynostratigraphic biozones in the Sydney, Gunnedah, Bowen, Galilee and Canning basins, Australia. Permophiles, v. 63, pp. 19–21.

Bogoslovskaya, M.F., 1962, Artinskian Ammonoids of the Central Urals: Proceedings of the Paleontological Institute of the Academy of Sciences of the USSR, v. 87 (Akad. Nauk SSSR, Moscow), pp. 3–117. (in Russian)

Bogoslovskaya, A.F., and Shkolin, A.A., 1998, Ammonoidea. In Grunt, T.A., Esaulova, N.K., and Kanev, G.P. eds. Biota of the East European Russia at the Early/Late Permian boundary: Moscow, Geos, pp. 137–155. (in Russian)

Buggisch, W., Wang, X.D, Alekseev, A.S., and Joachimski, M.M., 2011, Carboniferous–Permian carbon isotope stratigraphy of successions from China (Yangtze platform), USA (Kansas) and Russia (Moscow Basin and Urals). Palaeogeography, Palaeoclimatology, Palaeoecology, v. 301, pp. 18–38.

Cagliari, J., Schmitz, M.D., Lavina, E.L.C., and Netto, R.G., 2020, U-Pb CA-IDTIMS geochronology of the Late Paleozoic glacial and postglacial deposits in southern Paraná Basin. In EGU General Assembly 2020. doi:10.5194/egusphereegu2020-12101 [accessed 21th May 2020].

Chen, J., 2011, Early Permian (Cisuralian) conodont biostratigraphy in southern Guizhou and global correlation: PhD thesis, Graduate University of Chinese Academy of Sciences, Nanjing, 225 pp.

Chernykh, V.V., 2005, Zonal method in biostratigraphy, zonal conodont scale of the Lower Permian in the Urals. Institute of Geology and Geochemistry of RAN, Ekaterinburg, 217 p. (in Russian)

Chernykh, V.V., 2006, Lower Permian conodonts of the Urals. Institute of Geology and Geochemistry of RAN, Ekaterinburg, 130 p. (in Russian)

Chernykh, V.V., 2020, A brief review of the Dal'ny Tulkas Section (southern Urals, Russia) – potential candidate for a GSSP to define the base of the Artinskian stage in the global chronostratigraphic scale. Permophiles, v. 69, pp. 9–14.

Chernykh, V.V., and Chuvashov, B.I., 2004, Conodont biochronotype of Lower boundary of Sakmarian Stage. Annual-2003 of Institute of Geology and Geochemistry, Urals Branch of RAS. Ekaterinburg, UB RAS, pp. 28–33 (in Russian).

Chernykh, V.V., Chuvashov, B.I., Davydov, V.I., and Schmitz, M.D., 2012, Mechetlino Section: A candidate for the Global Stratotype and Point (GSSP) of the Kungurian Stage (Cisuralian, Lower Permian). Permophiles, v. 56, pp. 21–34.

Chernykh, V.V., Chuvashov, B.I, Davydov, V.I., Henderson, C.M., Shen, S., Schmitz, M.D., Sungatullina, G.M., Barrick, J.E., and Shilovsky, O.P., 2015, Southern Urals. Deep water successions of the Carboniferous and Permian. A Field Guidebook of XVIII International Congress on Carboniferous and Permian. Pre-Congress A3 Trip, August, 6-10, 2015. Kazan: Academy of Sciences of the Republic of Tatarstan Press, 88 p.

Chernykh, V.V., Chuvashov, B.I., Shen, S., Henderson, C.M., Yuan, D.X., and Stephenson, M.H., 2020, The Global Stratotype Section and Point (GSSP) for the base-Sakmarian Stage (Cisuralian, Lower Permian). Episodes, v. 43, pp. 961–979. doi:10.18814/epiiugs/2020/020059

Chuvashov, B.I., Chernykh, V.V., and Bogoslovskaya, M.F., 2002a, Biostratigraphic Characteristic of Stage Stratotypes of the Permian System. Stratigraphy and Geological Correlation, v. 10, pp. 317–333.

Chuvashov, B.I., Chernykh, V.V., Leven, E.Y., Davydov, V.I., Bowring, S., Ramezani, J., Glenister, B.F., Henderson, C.M., Schiappa, T.A., Northrup, C.J., Snyder, W.S., Spinosa, C., and Wardlaw, B.R., 2002b, Progress report on the base of the Artinskian and base of the Kungurian by the Cisuralian Working Group. Permophiles, v. 41, pp. 13–16.

Chuvashov, B.I., Chernykh, V.V., Shen, S., and Henderson, C.M., 2013, Proposal for the Global Stratotype Section and Point (GSSP) for the base-Artinskian Stage (Lower Permian): Permophiles, v. 58, pp. 26–34.

Chuvashov, B.I., Dyupina, G.V., Mizens, G.A., and Chernykh, V.V., 1990,

Reference sections of the Upper Carboniferous and Lower Permian of western flank Urals and Preurals. Academy of Sciences, USSR, 369 pp. (in Russian)

Davydov, V.I., Chuvashov, B., and Gareev, E., 2007, Report: Established and Proposed GSSPs of the Cisuralian Stages are Protected. Permophiles, v. 50, pp. 18–22.

Dehari, E., 2016, Upper Pennsylvanian–Lower Permian Carbonate Sedimentology and Conodont Biostratigraphy of the Strathearn and Buckskin Mountain formations, Carlin Canyon, Nevada [unpublished MSc thesis]: University of Calgary, Calgary, Alberta. 237 p.

di Pasquo, M., Grader, G.W., Isaacson, P., Souza, P.A., Iannuzzi, R., and Dıaz- Martınez, E., 2015, Global biostratigraphic comparison and correlation of an early Cisuralian palynoflora from Bolivia. Historical Biology, v. 27, pp. 868–897.

Filimonova, T.V., 2010, Smaller Foraminifers of the Lower Permian from Western Tethys. Stratigraphy and Geological Correlation, v. 18, pp. 687–811.

Foster, C.B., and Archbold, N.W., 2001, Chronologic anchor points for the Permian Early Triassic of the eastern Australian basins. *In* Weiss R.H. ed. Contributions to geology and palaeontology of Gondwana in honour of Helmut Wopfner. Geological Institute, University of Cologne, Germany, pp. 175–199.

Glenister, B.F., Baker, C., Furnish, W.M., and Dickins, J.M., 1990, Late Permian ammonoid cephalopod from Western Australia. Journal of Paleontology, v. 64, pp. 399–402.

Griffis, N.P., Montanez, I.P., Mundil, R., Richey, J., Isbell, J., Fedorchuk, N., Linol, B., Iannuzzi, R., Vesely, F., Mottin, T., Rosa, E., Keller, B., and Yin, Q.Z., 2019, Coupled stratigraphic and U-Pb zircon age constraints on the late Paleozoic icehouse-togreenhouse turnover in south-central Gondwana. Geology, v. 47, pp. 1146–1150.

Griffis, N.P., Mundil, R., Montanez, I.P., Isbell, J., Fedorchuk, N., Vesely, F., Iannuzzi, R., and Yin, Q.Z., 2018, A new stratigraphic framework built on U-Pb single zircon TIMS ages with implications for the timing of the penultimate icehouse (Paraná Basin, Brazil). Geological Society American Bulletin, v. 130, pp. 848–858.

Guerra-Sommer, M., Cazzulo-Klepzig, M., Menegat, R., Formoso, M.L.L., Basei, M.A.S., Barboza, E.G., and Simas, M.W., 2008a, Geochronological data from the Faxinal coal succession, southern Paraná Basin, Brazil: a preliminary approach combining radiometric U–Pb dating and palynostratigraphy. Journal of South American Earth Sciences, v. 25, pp. 246–256.

Guerra-Sommer, M., Cazzulo-Klepzig, M., Santos, J.O.S., Hartmann, L.A., Ketzer, J.M., and Formoso, M.L.L., 2008b, Radiometric age determination of tonsteins and stratigraphic constraints for the Lower Permian coal succession in southern Paranà Basin, Brazil. International Journal of Coal Geology, v. 74, pp. 13–27.

Guerra-Sommer, M., Cazzulo-Klepzig, M., Formoso, M.L.L., Menegat, R., and Mendonça, J.G., 2008c, U-Pb dating of tonstein layers from a coal succession of the southern Paraná Basin (Brazil): a new geochronological approach. Gondwana Research, v. 14, pp. 474–482.

Henderson, C.M., 1988, Conodont paleontology and biostratigraphy of the Upper Carboniferous to Lower Permian Canyon Fiord, Belcher Channel, Nansen, unnamed, and Van Hauen formations, Canadian Arctic Archipelago. Unpublished Ph.D. thesis, University of Calgary, Alberta, Canada, 287 pp.

Henderson, C.M., 1999, Correlation of Cisuralian and Guadalupian stages in the Sverdrup Basin, Canadian Arctic Archipelago. XIV ICCP. Pander Society. Can. Paleontol. Conf. Abstrs. Calgary, pp. 57–58.

Henderson, C.M., 2018, Permian conodont biostratigraphy. *In* Lucas, S.G. and Shen S.Z. eds. The Permian Timescale. Geological Society, London, Special Publication 450, pp. 119–142.

Henderson, C.M., 2020, Are we ready yet to propose a GSSP for base-Artinskian and base-Kungurian?. Permophiles, v. 69, pp. 23–26.

Henderson, C.M., and Chernykh, V.V., 2021, TO BE OR NOT TO BE *Sweetognathus asymmetricus*?. Permophiles, v. 70, pp. 10–13.

Henderson, C.M., Davydov, V.I., and Wardlaw, B.R., 2012, The Permian Period. *In* Gradstein, F.M., Ogg, J.G., Schmitz, M.D., and Ogg, G.M. eds. The Geological Timescale 2012, v. 2, Amsterdam, Elsevier, pp. 653–680.

Henderson, C.M., and McGugan, A., 1986, Permian conodont biostratigraphy of the Ishbel Group, southwestern Alberta and southeastern British Columbia. Contributian to Geology, University of Wyoming, v. 24. pp. 219–235.

Henderson, C.M., and Shen, S.Z., 2020, Chapter 24-The Permian Period. *In* Gradstein F.M., Ogg J.G., Schmitz M.D., and Ogg G.M. eds. The Geologic Time Scale 2020, Elsevier, v. 2, pp. 875–902.

Henderson, C.M., Schmitz, M., Crowley, J., and Davydov, V., 2009, Evolution and Geochronology of the *Sweetognathus* lineage from Bolivia and the Urals of Russia; Biostratigraphic problems and implications for Global Stratotype Section and Point (GSSP) definition. Permophiles, v. 53, Supplement 1, pp. 20–21.

Henderson, C.M., Wardlaw, B.R., Davydov, V.I., Schmitz, M.D., Schiappa, T.A., Tierney, K.E., and Shen, S.Z., 2012, Proposal for base-Kungurian. Permophiles, v. 55, pp. 8–34.

Holdsworth, B.K., and Jones, D.L., 1980, Preliminary radiolarian zonation for Late Devonian through Permian time. Geology, v. 8, pp. 281–285.

Holterhoff, P.F., Walsh, T.R., and Barrick, J.E., 2013, Artinskian (Early Permian) conodonts from the Elm Creek Limestone, a heterozoan carbonate sequence on the eastern shelf of the Midland Basin, West Texas, USA. *In* Lucas, S.G., Nelson, W.J. et al. eds. The Carboniferous–Permian Transition. New Mexico Museum of Natural History and Science Bulletin, v. 60, pp. 109–119.

Hounslow, M.W., and Balabanov, Y.P., 2018, A geomagnetic polarity timescale for the Permian calibrated to stage boundaries. *In* Lucas, S.G. and Shen S.Z. eds. The Permian Timescale. Geological Society, London, Special Publication 450, pp. 61–103.

Jurigan, I., Ricardi-Branco, F., Neregato, R., and Santos, T.J.S., 2019, A new tonstein occurrence in the eastern Paraná Basin associated with the Figueira coalfield (Parańa, Brazil): palynostratigraphy and U-Pb radiometric dating integration. Journal of South America Earth Science, v. 96, pp. 1–18.

Korte, C., Jasper, T., Kozur, H.W., and Veizer, J., 2006, ^{87}Sr/^{86}Sr record of Permian seawater. Palaeogeography, Palaeoclimatology, Palaeoecology, v. 240, pp. 89–107.

Kotlyar, G., Sungatullina, G., and Sungatullin, R., 2016, GSSPs for the Permian Cisuralian Series stages. Permophiles, v. 63. pp. 32–37.

Kozur, H., 1977, Beitrage zur Stratigraphie des Perms. Teil I. Probleme der Abgranzung und Gliederung des Perms. Freiberg. Forschungsheft, C334. Leipzig, pp. 85–161.

Lambert, L.L., Wardlaw, B.R., and Henderson, C.M., 2007, *Mesogondolella* and *Jinogondolella* (Conodonta): Multielement definition of the taxa that bracket the basal Guadalupian (Middle Permian Series) GSSP. Palaeoworld, v. 16, pp. 208–221.

Laurie, J.R., Bodorkos, S, Nicoll, R.S., Crowley, J.L., Mantle, D.J., Mory, A.J., Wood, G.R., Champion, D.C., Holmes, E., and Smith, T.E., 2016, Calibrating the middle and late Permian palynostratigraphy of Australia to the geologic time-scale via U–Pb zircon CA-IDTIMS dating. Australian Journal of Earth Sciences, v. 63, pp. 701–730.

Leonova, T.B., 1998, Permian ammonoids of Russia and Australia. Proceedings of the Royal Society of Victoria, v. 110, pp. 157–162.

Leonova, T.B., 2018, Permian ammonoid biostratigraphy. *In* Lucas, S.G. and Shen, S.Z. eds. The Permian Timescale. Geological Society, London, Special Publication 450, pp. 185–203.

Mei, S.L., Henderson C.M., and Wardlaw B.R, 2002, Evolution and distribution of the conodonts *Sweetognathus* and *Iranognathus* and related genera during the Permian, and their implications for climate change. Palaeogeography, Palaeoclimatology, Palaeoecology, v. 180, pp. 57–91.

Metcalfe, I., Crowley, J.L., Nicoll, R.S., and Schmitz, M., 2015, High-precision U-Pb CA-TIMS calibration of Middle Permian to Lower Triassic

sequences, mass extinction and extreme climate-change in Australian Gondwana. Gondwana Research, v. 28, pp. 61–81.

Mouro, L.D., Alves, M.L, Pacheco, F., Ricetti, J.H.Z., Scomazzon, A.K., Horodyski, R.S., Fernandes, A.C.S., Carvalho, M.A., Weinschutz, L.C., Silva, M.S., Waichel, B.L., and Scherer, C.M.S., 2020, Lontras Shale (Paraná Basin, Brazil): Insightful analysis and commentaries on paleo-environment and fossil preservation into a deglaciation pulse of the Late Paleozoic Ice Age. Palaeogeography, Palaeoclimatology, Palaeo-ecology, v. 555, pp. 109850, doi:10.1016/j.palaeo.2020.109850

Nassichuk, W.W., 1971, Permian ammonoids and nautiloids, south eastern Eagle Plain, Yukon Territory. Journal of Paleontology, v. 45, pp. 1001–1021.

Nassichuk, W.W., 1975, The stratigraphic significance of Permian ammonoids on Ellesmere Island. *In* Current Research, Part B, Geological Survey of Canada, pp. 277–283.

Nassichuk, W.W., Furnish, W.M., and Glenister, B.F., 1966, The Permian ammonoids of Arctic Canada; Geological Survey of Canada, Bulletin, v. 131, pp. 1–56.

Nazarov, B.B., 1988, Paleozoic Radiolaria. Practical Manual on Micro-fauna of the USSR. Nedra, Leningrad, 231 pp. (in Russian).

Nazarov, B.B., and Ormiston, A.R., 1985, Radiolarian from Late Paleo-zoic of the Southern Urals, USSR, and West Texas, USA. Micropale-ontology, v. 30, pp. 1–54.

Nazarov, B.B., and Ormiston, A.R., 1993, New biostratigraphically important Paleozoic Radiolaria of Eurasia and North America. Micropaleontol-ogy, Special Publication, v. 6, pp. 22–60.

Nestell, G.P., and Nestell, M.K., 2020, Roadian (earliest Guadalupian, Middle Permian) Radiolarians from the Guadalupe Mountains, West Texas, USA. Part I: Albaillellaria and Entactinaria. Micropaleontology, v. 66, pp. 1–50.

Nicoll, R., McKellar, J., Ayaz, S.A., Laurie, J., Esterle, J., Crowley, J., Wood, G., and Bodorkos S., 2015, CA-IDTIMS dating of tuffs, calibra-tion of palynostratigraphy and stratigraphy of the Bowen and Galilee basins. *In* Beeston J.W. ed. Bowen Basin and Beyond. Brisbane: Bowen Basin Symposium, 7-9 October 2015, pp. 211–218.

Park, S., 1989, Microfossils of the Permo-Carboniferous Strata of Non-gam Area in Mungyeong Coalfield. Journ. Korean Earth Science Soci-ety, v. 10, pp. 102–110.

Petryshen, W., Henderson, C.M., de Baets, K., and Jarochowska, E., 2020, Evidence of parallel evolution in the dental elements of *Sweetognathus* conodonts. Proceedings of the Royal Society B, 287, 20201922.

Price, P.L., 1997, Permian to Jurassic palynostratigraphic nomenclature of the Bowen and Surat basins. *In* Green P., ed. The Surat and Bowen Basins, southeast Queensland. Brisbane: Queensland Department of Mines and Energy, pp. 137–178.

Read, M.T., and Nestell, M.K., 2018, Cisuralian (Early Permian) Sweetog-nathid conodonts from the upper part of the Riepe Springs Limestone, north Spruce Mountain ridge, Elko County, Nevada. *In* Over, D.J and Henderson, C.M. eds. Conodont studies dedicated to the careers and contributions of Anita Harris, Glenn Merrill, Carl Rexroad, Walter Sweet, and Bruce Wardlaw. Bulletins of American Paleontology, v. 395–396, pp. 89–113.

Rhodes, F.H.T., 1963, Conodonts from the topmost Tensleep sandstone of the Eastern Big Horn Mountains, Wyoming. Journal of Paleontology, v. 37, pp. 401–408.

Riglos Suárez, M., Hünicken, M. A., and Merino, D., 1987, Conodont bio-stratigraphy of the Upper Carboniferous-Lower Permian rocks of Bolivia. *In* Austin, R.L. ed. Conodonts: investigative techniques and applica-tions, British Micropalaeontological Society, Ellis Horwood Publish-ers, London, pp. 317–325.

Ritter, S. M., 1986, Taxonomic revision and Phylogeny of post-early crisis *bisselli-whitei* Zone conodonts with comments on Late Paleozoic diversity. Geologica et Palaeontologica, v. 20. pp. 139–165.

Rocha-Campos, A.C., Basei, M.A.S., Nutman, A.P., and Santos, P.R., 2006, SHRIMP U-Pb zircon geochronological calibration of the late Paleo-

zoic Supersequence, Paraná Basin, Brazil. In: South American Sympo-sium on Isotope Geology, pp. 322–325. doi:10.1111/iar.12220

Rocha-Campos, A.C., Basei, M.A.S., Nutman, A.P., and Santos, P.R., 2007, SHRIMP U-Pb zircons ages of the late Paleozoic sedimentary sequence, Parana Basin, Brazil. *In*: Simposio sobre Cronoestratigrafia da Bacia do Paraná, 4, 2007, Rio de Janeiro, Boletim de Resumos, p. 33.

Rocha-Campos, A.C., Basei, M.A.S., Nutman, A.P., Santos, P.R., Pas-sarelli, C.R., Canile, F. M., Rosa, O.C.R., Fernandes, M.T., Santa Ana, H., and Veroslavsky, G., 2019, U-Pb zircon dating of ash fall deposits from the Paleozoic Paraná Basin of Brazil and Uruguay: a reevaluation of the stratigraphic correlations. Jornal of Geology, v. 127, pp. 167–182.

Ruzhencev, V.E., 1956, Lower Permian ammonites of the Urals – Ammo-nites of the Artinskian Stage. Trudy Paleontologicheskogo Instituta Akademii Nauk SSSR, v. 60, pp. 1–271.

Santos, R.V., Souza, P.A., Alvarenga, C.J.S., Dantas, E.L., Pimentel, M.M., Oliveira, C.G., and Araujo, L.M., 2006, Shrimp U-Pb zircon dating and palynology of bentonitic layers from the Permian Irati Formation, Paranà basin, Brazil. Gondwana Research, v. 9, pp. 456–463.

Schiappa, T.A., Hemmesch, N.T., Spinosa, C., and Nassichuk, W.W., 2005, Cisuralian ammonoid genus *Uraloceras* in North America. Journal of Paleontology, v. 79, pp. 366–377.

Schmitz, M.D., and Davydov V.I., 2012, Quantitative radiometric and bio-stratigraphic calibration of the Pennsylvanian–Early Permian (Cisura-lian) time scale and pan-Euramerican chronostratigraphic correlation. GSA Bulletin, v. 124, pp. 549–577.

Schmitz, M.D., Davydov, V.I., and Snyder, W.S., 2009, Permo-Carbonif-erous Conodonts and Tuffs: High precision marine Sr isotope geochro-nology. Permophiles, v. 53, Supplement 1 (ICOS 2009 Abstracts edited by C.M. Henderson and C. MacLean), pp. 48.

Scomazzon, A.K., Wilner, E., Purnell, M.A., Nascimento, S., Weinschütz, L.C., Lemos, V.B., de Souza, F.L., and da Silva, C.P., 2013, First report of conodont apparatuses from Brazil – Permian of Paraná Basin, Itararé Group, Lontras Shale – Evidence of Gondwana deglaciation. In: Cono-dont from the Andes. 3rd International Conodont Symposium. Publi-cación Especial N°13. Paleontological Note, pp. 99–102.

Shen, S.Z., Wang, Y., Henderson, C.M., Cao, C.Q., and Wang, W., 2007, Biostratigraphy and lithofacies of the Permian System in the Laibin-Heshan area of Guangxi, South China. Palaeoworld, v. 16, pp. 120–139.

Simas, M.W., Guerra-Sommer, M., Cazzulo-Klepzig, M., Menegat, R., Schneider Santos, J.O., Fonseca Ferreira, J.A., and Degani-Schmidt, I., 2012, Geochronological correlation of the main coal interval in Brazil-ian Lower Permian: radiometric dating of tonstein and calibration of biostratigraphic framework. Journal of South American Earth Science, v. 39, pp. 1–15.

Stewart, J.H., Murchey, B., Jones, D.L., and Wardlaw, B.R., 1986, Paleon-tologic evidence for complex tectonic interlayering of Mississippian to Permian deep-water rocks of the Golconda allochthon in Tobin Range, north-central Nevada. Geological Society of America Bulletin, v. 97, pp. 1122–1132.

Souza, P.A., Boardman, D.R., Premaor, E., Félix, C.M., Bender, R.R., and Oliveira, E.J., 2021, The *Vittatina costabilis* Zone revisited: New char-acterization and implications on the Pennsylvanian-Permian icehouse-to-greenhouse turnover in the Paraná Basin, Western Gondwana, Journal of South American Earth Sciences, v. 106, doi:10.1016/j.jsames.2020.102968

Stephenson, M.H., 2007, Preliminary results of palynological study of the Dal'ny Tulkas section, location of the proposed basal Artinskian GSSP. Permophiles, v. 50, pp. 22–25.

Stephenson, M.H., 2016, Permian palynostratigraphy: a global overview. *In* Lucas, S.G., and Shen, S.Z. eds. The Permian Timescale. Geological Society, London, Special Publications, v. 450, pp. 321–347. doi:10.1144/SP450.2

Suarez-Riglos, M., Hunicken, M.A., and Merino-Rodo, D., 1987, Cono-dont biostratigraphy of the Upper Carboniferous–Lower Permian rocks of

Bolivia. *In* Austin RL, editor. Conodonts: investigative techniques and applications. British Micropalaeontological Society. London: Ellis Horwood Publishers, pp. 317−325.

Sun, Y.D., Liu, X.T., Yan, J.X., Li, B., Chen, B., Bond, D.P.G. et al., 2017, Permian (Artinskian to Wuchiapingian) conodont biostratigraphy in the Tieqiao section, Laibin area, South China. Palaeogeography, Palaeoclimatology, Palaeoecology, v. 465, pp. 42−63.

Wang, C.Y., Ritter, S.M., and Clark, D.L., 1987, The *Sweetognathus* complex in the Permian of China: implications for evolution and homeomorphy. Journal of Paleontology, v. 61, pp. 1047−1057.

Wang, Z.H., and Higgins, A.C., 1989, Conodont zonation of the Namurian--Lower Permian strata in South Guizhou, China. PalaeontoIogia Cathayana, v. 4, pp. 261−325.

Wang, Z.H., 1994, Early Permian conodonts from the Nashui section, Luodian of Guizhou. Palaeoworld, v. 4, pp. 203−224.

Wardlaw, B.R., and Nestell, M.K., 2015, Conodont faunas from a complete basinal succession of the upper part of the Wordian (Middle Permian, Guadalupian, West Texas). Micropaleontology, v. 61, pp. 257−292.

Wood, G.D., Gabriel, A.M., and Lawson, J.C., 1996, Palynological techniques – processing and microscopy. *In* Jansonius, J., and McGregor, D.C. eds. *Palynology: Principles and Applications*. American Association of Stratigraphical Palynologists Foundation, v. 1, pp. 29−50.

Zeng, J., Cao, C.Q., Davydov, V.I., and Shen, S.Z., 2012, Carbon isotope chemostratigraphy and implications of paleoclimatic changes during the Cisuralian (Early Permian) in the southern Urals, Russia. Gondwana Research, v. 21, pp. 601−610.

Zhang, L., Feng, Q.L., and He, W.H., 2018, Permian radiolarian biostratigraphy. *In* Lucas, S.G. and Shen, S.Z. eds. The Permian Timescale. Geological Society, London, Special Publication 450, pp. 143−163.

Zhang, Z.H., Wang, Z.H., and Li, C.Q., 1988, Permian strata in South Guizhou. 1−113, Guiyang (in Chinese).

Valery V. Chernykh received his Ph. D. from the Mining Institute of the Geological Faculty in Sverdlovsk. He has worked in the Institute of Geology and Geochemistry of the Ural Branch of the Russian Academy of Science since 1981. He presently holds the position of lead scientist in the Laboratory of Stratigraphy and Paleontology. His research interests include evolutionary biology, micropaleontology, and stratigraphy. His current research focuses on Permian stratigraphy and micropaleontology of the Ural Mountains. He has published more than 200 works, including seven monographs.

Michael H. Stephenson is an independent palynologist, stratigrapher and geologist. He is Director of Stephenson Geoscience Consulting Ltd., Director of the IUGS Deep-time Digital Earth program, Expert Associate of TÜV Nord Ltd., Vice-Chair of the Subcommission on Permian Stratigraphy, visiting professor at Nanjing and Milan universities and the Karakoram International University, and Research Associate at the British Geological Survey. He has published more than 100 peer-reviewed scientific papers and three widely regarded popular books on geoscience. He has delivered high profile lectures, for example in the UK Parliament, and has been a science advisor for the BBC's 'Horizon', 'Bang Goes the Theory' and 'Holby City' programmes.

Charles M. Henderson is a Professor at the University of Calgary where he has taught stratigraphy and paleontology since 1989. His primary research is on the biostratigraphy of Permian and Early Triassic conodonts around the world, including in arctic and western Canada, China, Oman, Bolivia, Russia, and the United States. His research is focused on the completion of a global chronostratigraphic subdivision of the Permian System. He is a Fellow of The Royal Canadian Geographical Society and the Geological Society of America and former Chairman of the Subcommission on Permian Stratigraphy, ICS.

Lucia Angiolini is a Professor at the University of Milano, Italy where she has taught paleontology, paleocology and biomineralization for more than 20 years. Her primary research is on the taxonomy and biostratigraphy of Carboniferous and Permian brachiopods from N Europe, the Mediterranean region, N Africa, Arabia and Asia. Her research is also focused on the paleoclimatological and paleoecological implications of the study of Paleozoic brachiopods. She is the current Chair of the Subcommission on Permian Stratigraphy, ICS and former President of the Società Paleontologica Italiana.